Alaska Earthquake Source for the SAFRR Tsunami Scenario

Open-File Report 2013–1170–B
California Geological Survey Special Report 229

U.S. Department of the Interior
U.S. Geological Survey

COVER: Early map of Alaska Territory (in Gaskell's New and Complete Family Atlas of the World), 1896

The SAFRR (Science Application for Risk Reduction) Tsunami Scenario

Stephanie Ross and Lucile Jones, Editors

Alaska Earthquake Source for the SAFRR Tsunami Scenario

By Stephen Kirby, David Scholl, Roland von Huene, and Ray Wells

Open-File Report 2013–1170–B

California Geological Survey Special Report 229

U.S. Department of the Interior
U.S. Geological Survey

U.S. Department of the Interior
SALLY JEWELL, Secretary

U.S. Geological Survey
Suzette M. Kimball, Acting Director

U.S. Geological Survey, Reston, Virginia 2013

For product and ordering information:
World Wide Web: http://www.usgs.gov/pubprod
Telephone: 1-888-ASK-USGS

For more information on the USGS—the Federal source for science about the Earth, its natural and living resources, natural hazards, and the environment:
World Wide Web: http://www.usgs.gov
Telephone: 1-888-ASK-USGS

Suggested citation:
Kirby, S., Scholl, D., von Huene, R., and Wells, R., 2013, Alaska earthquake source for the SAFRR tsunami scenario, chap. B, *in* Ross, S.L., and Jones, L.M., eds., The SAFRR (Science Application for Risk Reduction) Tsunami Scenario: U.S. Geological Survey Open-File Report 2013–1170, 40 p., http://pubs.usgs.gov/of/2013/1170/b/.

STATE OF CALIFORNIA
EDMUND G. BROWN JR.
GOVERNOR

THE NATURAL RESOURCES AGENCY
JOHN LAIRD
SECRETARY FOR RESOURCES

DEPARTMENT OF CONSERVATION
MARK NECHODOM
DIRECTOR

CALIFORNIA GEOLOGICAL SURVEY
JOHN G. PARRISH, Ph.D.
STATE GEOLOGIST

Acknowledgments

We are grateful for the help, guidance, and advice provided by the generosity of the following colleagues: Contributing U.S. Geological Survey (USGS) Tsunami Source Working Group members (TSWG): Holly Ryan, Rick Blakely, Stephanie Ross, George Plafker, Eric Geist, Willie Lee, Emily Roland, Amy Draut, Guy Gelfenbaum, and Walter Mooney; other USGS: Gavin Hayes (Golden, Colo.), Alan Nelson (Golden), and John Miller (Denver, Colo.); California Geological Survey: Rick Wilson. We appreciate the support of the following in tsunami modeling: Hong Kie Thio (URS Corp.); Roger Hansen, Elena Suleimani, and Dmitri Nicolsky (all Geophysical Institute of the University of Alaska at Fairbanks; Aggeliki Barberopoulou (University of Southern California); the 2011 Tohoku earthquake slip modelers, especially Thorne Lay (University of California Santa Cruz), Chen Ji (University of California Santa Barbara), Mark Simons (California Institute of Technology), Sarah Minson (Formerly at California Institute of Technology and now at the U.S. Geological Survey in Seattle), Y. Ito and T. Iinuma (both at Tohoku University). We are grateful also for advice and discussions in Japan with Ryota Hino, Dapeng Zhao, Toru Matsuzawa, and Akira Hasegawa (all at Tohoku University); Douglas Christenson, Jeff Freymueller, and Roger Hansen (all at the Geophysical Institute of the University of Alaska at Fairbanks); Emile Okal (Department of Earth and Planetary Sciences, Northwestern University). We thank Eleyne Phillips (USGS) for geographic information system construction and images and Peter Stauffer (USGS, Menlo Park) for his helpful edit.

Contents

Alaska Earthquake Source for the SAFRR Tsunami Scenario

By Stephen Kirby, David Scholl, Roland von Huene, and Ray Wells

"What *did* happen can happen again [elsewhere]"
– Paraphrased aphorism

"Extreme events can and do happen…"
– Thorne Lay and Hiroo Kanamori, Physics Today, 2011

"Hope for the best, but prepare for the worst."
– An oft-quoted adage.

Abstract

Tsunami modeling has shown that tsunami sources located along the Alaska Peninsula segment of the Aleutian-Alaska subduction zone have the greatest impacts on southern California shorelines by raising the highest tsunami waves for a given source seismic moment. The most probable sector for a $M_w \sim 9$ source within this subduction segment is between Kodiak Island and the Shumagin Islands in what we call the Semidi subduction sector; these bounds represent the southwestern limit of the 1964 M_w 9.2 Alaska earthquake rupture and the northeastern edge of the Shumagin sector that recent Global Positioning System (GPS) observations indicate is currently creeping. Geological and geophysical features in the Semidi sector that are thought to be relevant to the potential for large magnitude, long-rupture-runout interplate thrust earthquakes are remarkably similar to those in northeastern Japan, where the destructive M_w 9.1 tsunamigenic earthquake of 11 March 2011 occurred.

In this report we propose and justify the selection of a tsunami source seaward of the Alaska Peninsula for use in the Tsunami Scenario that is part of the U.S. Geological Survey (USGS) Science Application for Risk Reduction (SAFRR) Project. This tsunami source should have the potential to raise damaging tsunami waves on the California coast, especially at the ports of Los Angeles and Long Beach. Accordingly, we have summarized and abstracted slip distribution from the source literature on the 2011 event, the best characterized for any subduction earthquake, and applied this synoptic slip distribution to the similar megathrust geometry of the Semidi sector. The resulting slip model has an average slip of 18.6 m and a moment magnitude of $M_w = 9.1$. The 2011 Tohoku earthquake was not anticipated, despite Japan having the best seismic and geodetic networks in the world and the best historical record in the world over the past 1,500 years. What was lacking was adequate paleogeologic data on prehistoric earthquakes and tsunamis, a data gap that also presently applies to the Alaska Peninsula

and the Aleutian Islands. Quantitative appraisal of potential tsunami sources in Alaska requires such investigations.

Introduction

Background

Tsunami modeling has shown that the most effective subduction earthquakes for raising tsunami waves along southern California shorelines are those that occur offshore of the Alaska Peninsula (Thio and others, 2010; fig. 1). We review the instrumental and preinstrumental record of seismicity in that region and conclude that the previous cumulative seismic slip in the instrumental history in the Semidi sector, which we define as between Kodiak Island and the Shumagin Islands, is small. Although nearby subduction sectors have generated great and giant tsunamigenic earthquakes in 1946 and 1964, those earthquakes did not cause damaging tsunami waves along southern California shorelines, largely because of their different trench azimuths and positions and differences in tsunami wave-field directivity and in sea-floor bathymetry between source and receiving shoreline. For a giant earthquake ($M_w \geq 8.5$), the Semidi subduction sector may therefore be the optimum subduction sector for producing tsunami waves along southern and central California shorelines.

The *M*9.1 Tohoku subduction earthquake of 11 March 2011 changed the way that many earthquake scientists think about subduction earthquakes and their tsunami effects. First, the 2011 event was not anticipated because of the lack of historical information about previous earthquakes of this size. Although an earthquake that occurred in the year 869 produced large runups along Sendai Bay (Minoura and others, 2001), paleotsunamic evidence is lacking farther north along the Sanriku coast (Sugawara and others, 2011, unpublished field guide on the Jogan and 2011 Tohoku tsunami deposits). Based on this limited known length of tsunami effects in AD 869, tsunami modeling showed that a source magnitude of 8.1 to 8.3 adequately explained the runups and inundations suggested by the paleotsunamic record (Satake and others, 2007). Therefore the historical record in Japan, even though it is among the longest for any region on Earth, was inadequate to have anticipated an earthquake of the magnitude of the 2011 event. More prehistoric information on subduction earthquakes and tsunamis was clearly needed, such as has been found in Cascadia and the eastern Gulf of Alaska subduction sectors. Secondly, on-land Global Positioning System (GPS) data did not have sufficient resolution to determine that the locking on the Japan Trench subduction margin extended to the Japan Trench. Thirdly, Tohoku University and the Japan Agency for Marine-Earth Science (JAMSTEC), and other Japanese partners installed sea-floor GPS instruments, pressure gages, tsunami wave meters, and cabled sea-floor instruments in the source region before the 11 March 2001 earthquake. Analysis of those data indicated that extraordinarily high maximum slip occurred during the earthquake rupture near the trench, as large as 80 m. Without this sea-floor instrumentation, the true nature of this tsunami source would not have been revealed.

The above considerations indicate that for earthquakes of this moment magnitude, events with compact rupture areas and large associated average and peak slip probably occur on time scales of thousands of years (Satake, 2011). Historical and instrumental information are consequently inadequate to establish the likelihood of the occurrence of such events. Scientists tasked with considering tsunami hazards and risks must therefore ask the question—could such a tsunamigenic earthquake occur in “my” subduction zone (McCaffrey, 2007, 2008)?

Our Charge

The purpose of this report is to summarize briefly and justify the selection of a tsunami source seaward of the Alaska Peninsula for use in the Tsunami Scenario that is part of the U.S. Geological Survey (USGS) Science Application for Risk Reduction (SAFRR) Project. Our charge was to propose a tsunami source offshore of the Alaska Peninsula that had the potential to raise damaging tsunami waves along California coastlines, especially at the ports of Los Angeles and Long Beach. This source needed to be credible and plausible in light of the state of knowledge in early 2012, when this tsunami source scenario was formulated, and to represent an event that could occur sometime in the future. Being the most likely next large tsunami source for southern California shorelines was not a requirement. The specific source presented in this report was described and discussed on 27 February 2012 at the USGS facilities in Menlo Park, California, by participating members of the USGS Tsunami Source Working Group—Stephanie Ross, Scenario Manager for SAFRR, David Scholl, Ray Wells, Rick Blakely, Roland von Huene, Willie Lee, Walter Mooney, Amy Draut, and Tracy Vallier (all USGS); Rick Wilson (California Geological Survey); and Roger Hansen (Geophysical Institute at the University of Alaska at Fairbanks, GI/UAF). Other participants on conference call for this meeting were Hong Kie Thio (URS Corporation), George Choy (USGS, Golden, Colo.), Elena Suleimani and Dmitry Nicolsky (GI/UAF), Lucy Jones (USGS, Pasadena), Kenny Ryan (University of California Riverside), David Lockner and Tom Brocher (both USGS Earthquake Science Center) and Dale Cox (USGS, Pasadena). After discussion of the proposed source, the participants offered no alternatives and, when specifically asked, there were no objections to the scenario being put forward as the official USGS SAFRR Tsunami Scenario model. The model was also discussed in presentations by Kirby at Tohoku University in May 2012 and at the University of Alaska Geophysical Institute in February 2012, where opportunities for questions and comments were both offered and exercised.

In this source selection, we chose to apply a Tohoku-type tsunami source because of strong similarities in the geologic and geophysical frameworks of the Semidi and Tohoku subduction sectors, similarities that we summarize in this report. We do not claim that this source has the highest probability among possible future great and giant tsunamigenic earthquakes. Such probability cannot be assessed without comprehensive paleoseismic and paleotsunamic surveys in the Semidi sector. Lacking such information, our goal is to posit a M_w~9 tsunami source that could plausibly occur at some time in the future based on the similarities in framework geology and geophysics between the Semidi and Tohoku subduction segments. Put another way, is such a source plausible given our present state of knowledge or lack of knowledge? We not only lack sufficient prehistoric data on the Semidi sector on average recurrence times, but we also do not know how late we are in the average giant earthquake return time and how much stored slip has accumulated. It cannot be claimed with any confidence that the probability of a compact, high-average-slip tsunamigenic earthquake is impossibly low in the Semidi segment. The same could have been said, but was not, about the likelihood of a giant subduction earthquake in the southern Tohoku subduction margin on 10 March 2011, just prior to the catastrophe that occurred one day later.

Plan of This Report

Our plan for this report is to first review the tectonic setting and the history of seismicity and tsunami generation on the subduction zone in the Pacific offshore the Alaska Peninsula. Secondly, we compare the geological and geophysical frameworks of the Tohoku and Semidi subduction segments and evaluate whether their similarities outweigh their differences. Thirdly, we abstract from the numerous slip models for the 2011 Tohoku earthquake a simplified synoptic slip model that we apply to a three-dimensional (3-D) model for the geometry of the Semidi-segment of the megathrust boundary, which was found very similar to that of the Tohoku segment. We explain briefly how the geometrical subfault model was constructed and how we populated that array with coseismic slip. Fourthly, we discuss the subject of scaling of rupture sizes and average slip with scalar seismic moment and moment magnitude for subduction earthquakes in light of the inadequacy of the existing seismic record for giant subduction earthquakes (M_w>8.5), and we discuss challenges in using a scaling law as a guide to earthquake sources in this seismic moment range. Finally, the 3-D slip distribution for the tsunami scenario source will be provided in a spreadsheet that may be found in an appendix as supplemental information. In the interest of making this report as brief as possible, we summarize relevant information as much as is practical in tables. The information sources that we used in producing the Semidi sector slip model were largely limited to those available as of 25 January 2012, but they include final publication citations that were previously available only in abstract.

Tectonic Setting and the Instrumental, Historical, and Prehistoric Seismic and Tsunamic Record of the Semidi Sector

The following account includes events in the Semidi sector and nearby segments of the Aleutian-Alaska subduction zone (table 1). It also reviews the maximum tsunami wave heights produced by earthquakes in this segment at key Pacific coastal locations, especially in California (National Geophysical Data Center, 2012; Novosibirsk Tsunami Laboratory, 2012).

The M_w 8.2 to 8.3 Subduction Earthquake of 10 November 1938

The instrumental history of the Semidi sector for events with M>7 and of great earthquakes in nearby segments is summarized in table 2 and illustrated in figures 2a, 3b, and 4a. The 1938 main-shock epicenter places it near the Slab 1.0 interface at depths between 20 and 40 km (table 1). (Slab 1.0 is a global 3-D slab geometry model based on the hypocenters of interplate thrust earthquakes and subduction plate boundary information from seismic reflection profiles—see Hayes and others, 2012). The relocated 1-month aftershocks of the 1938 event (Emile Okal, written commun., 2010) cover most of the Semidi sector, nearly out to the trench. Although the 10 November 1938 earthquake was an M_w 8.2–8.3 event, recorded wave heights are all less than 0.3 m and tsunami modeling of its small regional and far-field tsunami waves indicate that its three slip patches had an average slip of about 1.1 to 2.1 m and a maximum slip of 3.3 m in the easternmost subfault (Johnson and Satake, 1994, 1995). An independent seismic waveform analysis also indicates that average slip was about 2 m (Estabrook and others, 1994). These are very small slips in light of cumulative relative plate motion in the Semidi sector since 1938 (about 4.5 m) and the potential for large stored slip prior to the instrumental era.

All told, the small number of other large instrumentally documented earthquakes (figs. 2a, 3b, and 4) indicates that a very small release of accumulated slip has occurred in the century plus of plate motion since the beginning of global seismology in about 1899. During this period more than 6.8 m of plate motion occurred. None of the great earthquakes in adjoining sectors or the 1938 event have produced recorded tsunami waves in southern California greater than 1.1 m (table 1).

Gulf of Alaska Sector

The *M* 9.2 to 9.3 earthquake of 28 March 1964 was the largest instrumentally recorded earthquake in Alaska and the second largest in the global instrumental record (International Seismological Center, 2013). The four published inversions of geodetic and seismic data for slip-accumulation distribution, although differing in data selection, methodology, and details of the resultant slip inversion, all recognize two patches of large slip, one under the Prince William Sound area and one trenchward of Kodiak Island and the pass southwest of the Kenai Peninsula and northeast of Kodiak Island (Holdahl and Sauber, 1993; Christensen and Beck, 1994; Johnson and others, 1996; Ichinose and others, 2007; Suito and Freymueller, 2009). This pattern is also consistent with the aftershock distribution. Ichinose and others (2007) also subdivided the Prince William Sound patch into two subfaults and verified the trenchward Kodiak slip region. These findings and other considerations suggest that as a conservative approach, the northeast limit of the SAFRR tsunami scenario source should not extend under the Kodiak subduction sector, because it represents rupture for a relatively recent earthquake.

The M_w 8.6 Unimak Island/Sanak Island Earthquake of 1 April 1946

This shock (see fig. 2a) was unusual in several related respects: it was generally deficient in high-frequency energy, its epicenter was very near the Aleutian Trench, and it had unusually high potency as a tsunami source both in the near and far fields (Kanamori, 1972; Johnson and Satake, 1997, Okal and others, 2002, 2003; Lopéz and Okal, 2006). Its tsunami magnitude was 9.3 (Abe, 1979). It was one of the first earthquakes identified as being of the “tsunami” earthquake category that produces outsized tsunami waves compared to their conventional moment magnitudes (Kanamori, 1972). The average slip was about 8 m or more as estimated by López and Okal (2006). The directivity of tsunami waves from this source toward Hawaii made it particularly destructive. There are similarities in the geologic frameworks of the southwest Alaska Peninsula continental slope where the 1946 earthquake occurred and the Semidi sector

(Bruns and others, 1987) that suggest that a component of slow-rupture, high-near-trench slip could also occur in the Semidi sector (von Huene and others, 2012).

Regional Stored Slip Accumulations Based on GPS Observations.

Freymueller and Beavan (1999); Fletcher and others (2001); Fournier and Freymueller (2007), Freymueller and others (2008), and Cross and Freymueller (2008) have described the results of Global Positioning System (GPS) observations in Alaska. Their analyses indicate that the region northeast of the Shumagin Islands is presently “locked” and has been accumulating stored slip, In contrast, the southwest offshore sector of the Alaska Peninsula, which includes the Shumagin Islands, is probably creeping, although resolution is thought to be poor for the subduction boundary near the trench far from the nearest GPS instruments. However, we do not know whether this creeping condition represents the long-term way that subduction motion is accommodated in the Shumagin sector. These same locked versus creeping conclusions about these two sectors adjacent to the Semidi sector were adopted as inputs in the most current USGS probabilistic seismic hazard map for the State of Alaska (Wesson and others, 2007) and we adhere to their assessment.

Historical Record for Tsunamigenic Earthquakes in the Semidi Sector: the 1788 Event and the Purported Tsunamigenic 1847–1848 Earthquake

Russian information on earthquake occurrence and seismic intensities and tsunami inundations in Alaska prior to the Territory’s purchase by the United States in 1867 is typically fragmentary, mostly recorded long after the event by those who were not eyewitnesses and citing observations at sparse locations. Even event dates are unclear from this incomplete record.

July/August 1788.—A short few years after Russian long-term settlement began on the Alaska Peninsula and its offshore islands, two events occurred in that region. The sources of information (see Davies and others, 1981; Sykes and others, 1981) on these events are the following. (1) W. Merkul’ev (b.?; d.1828), a warehouse manager on Kodiak Island at the time of the 22 August 1788 earthquake and tsunami: He wrote a letter shortly after the events, describing them to his boss, Grigory Ivanovich Shelekhov (1747–1786), cofounder of the Shelekhov-Golikov Company. (2) G.I. Davydov, who was in Alaska in the first decade of the 19th century: His accounts were published in English in 1813. (3) Russian Orthodox priest Ioann (Father John) Veniaminov (1797–1879), who was in Alaska from 1824 to about 1840: His diary was published in 1840. (4) Geologist Pëtr Pavlovich Doroshin (1823–1875), who arrived in Russian Alaska in 1848 and wrote of his experience in a report that was published in 1870. Only Merkul’ev was an eyewitness. The others collected information decades after the events, and those impressions and descriptions were published decades after collection. Not surprisingly, there is confusion as to the exact dates of these events and which events preceded others. The experiences of Merkul’ev on 22 July (in the present-day Gregorian calendar) describing the strong earthquake ground motions and tsunami inundations at Three Saints Harbor, located in a fjord on the south coast of Kodiak Island, carry the most weight because they are first-hand and written shortly after the events. In reviewing all of these records, S.L. Soloviev (1968; English translation published 1990) implies in his figure 1 that there was one giant earthquake that ruptured about 650 km of the Alaska Peninsula margin from south of Kodiak to Sanak Island. This source model seems very unlikely because of the insistence by Veniaminov, a keen interviewer and native-language interpreter, that big tsunami waves occurred on Unga and Sanak Islands on 7 August (again according to the present-day Gregorian calendar), 16 days after the 22 July earthquake and tsunami waves reported by Merkul'ev.

Another possibility was raised by Emile Okal (written commun., 2011) that a large earthquake occurred on 22 July somewhere along the subduction margin between the Gulf of Alaska and Sanak Island and that 16 days later, on 7 August, a large submarine landslide occurred near the southwest end of the Alaska Peninsula that was triggered as a delayed response by the ground motions of the earlier 22 July earthquake. According to this model, it was this localized submarine landslide tsunami source that flooded the settlement on Unga and destroyed livestock on Sanak Island, both to levels up to a few tens of meters above sea level. Okal's interpretation is strengthened by recent geophysical investigations of the continental slope southwest of the Shumagin Islands that reveal morphological evidence for large submarine slumps near the southern edge of the continental shelf (Roland von Huene, unpublished swath-map image, 2013).

Okal's hypothesis seems to satisfy most of the historical records that might be judged reliable, including the lack of evidence for strong earthquake ground motions on 7 August. We are left with a large earthquake occurring somewhere off the Alaska Peninsula on 22 July 1788 that was large enough to raise waves 3–10 m high at the old harbor in Three Saints Bay, Kodiak (a narrow fjord) and produced at least localized strong ground motions and sustained aftershocks at that locality. As to its seismic moment, area of rupture, and average slip, we lack adequate information to go further. Any assumption that the 1788 event(s) resulted in complete release of stored interplate slip is unsupported by the sparse evidence summarized above. Without such an assumption, the present-day state of stored interplate slip cannot be estimated. A continuing search for 1788 tsunami deposits on ocean-facing embayments along the Pacific side of the Alaska Peninsula and its islands may resolve some of the questions about this earthquake and the tsunami waves that it produced.

1847/1848—This "event," cited in Davies and others (1981), is extremely doubtful (Lander and Lockridge, 1989). It is based on an historical account of a strong "orphan" tsunami in Tahiti, the source of which is now unclear because Tahiti is not a plate-boundary tsunami source. The same authors suggest that tsunami waves of similar potency occurred in Hawaii in the mid-to-late 1840's. Although earthquakes were felt in early morning of 15 April 1848 off the Alaska Peninsula at Chirikof and Unga Islands, no report of tsunami waves are known by the authors of the present report for that part of Alaska on any date in the years 1847 or 1848. Moreover, none of the other qualified compilers of tsunami events and large earthquakes in the modern era recognize this "event" as valid for Alaska (Lander, 1996; Novosibirsk Tsunami Laboratory, 2012; Pararas-Carayannis and Calebaugh, 1977; Brockman and others, 1988; Lander and Lockridge, 1996).

We conclude from this historical record of tsunamigenic earthquakes that an unknown amount of seismogenic slip occurred in July and possibly August 1788. The lack of historical and instrumental evidence for a large area of tsunamigenic slip (>4 m) since then suggests that cumulative historical seismogenic slip release has been small.

Clearly information on prehistoric tsunamigenic earthquakes in the Semidi sector is needed for future guidance on the likelihood of a giant tsunamigenic earthquake.

The Paleogeologic Record.

Just a few short years ago, Gary Carver and George Plafker wrote that paleogeologic investigations of subduction earthquakes were largely restricted to the Gulf of Alaska subduction sector (Carver and Plafker, 2008). This situation has changed greatly in the past 5 years through partnerships between USGS scientists—largely supported by the USGS Multihazards Demonstration Project (MHDP), by SAFRR (the successor of MHDP), and by the Alaska Earthquake Hazards Project, and university scientists supported largely by the National Science Foundation (NSF) and the USGS, and a geologist with the State of Alaska Division of Geological and Geophysical Surveys. Over the last several summer seasons, field surveys have visited Chirikof Island, Sitkinak Island near Kodiak, and Simeonof Island in the southeast Shumagin Islands.

Results from these surveys so far are preliminary and unpublished, and correlations between islands are not yet confidently identified. Alan Nelson (USGS, Golden) and others have compiled what is known so far (unpublished report, 2012). However, the initial findings are encouraging at two of these sites, one on Chirikof and one on Sitkinak. These investigators have dated possible and probable tsunami deposits and evidence for elevation changes possibly caused by large subduction earthquakes. Intervals between dated events vary greatly—from as little as one hundred to a few hundred years up to many hundreds to 1,300 years. At the long end of these interevent intervals, slip accumulations of many tens of meters are possible.

Preliminary findings from geologic field work on Simeonof Island in the Shumagin Islands imply little strain accumulation and release on the Aleutian-Alaska megathrust beneath the Shumagin Islands in the past 3,400 years (Witter and others, 2012). These initial paleogeologic results provide support for the interpretation of GPS observations summarized earlier in this report that the Shumagin sector is largely slipping aseismically and that the western limit of rupture for scenario models should not include the Shumagin sector.

As embayments, salt marshes, and tidal flats are investigated on more and more islands, such as Sanak Island southwest of the Shumagins and Unga Island in the Shumagins, and onshore along the Pacific coast of the Alaska Peninsula, we should have a fuller picture of the chronology of prehistoric megathrust earthquake occurrence in the offshore of the Alaska Peninsula. In the meantime, we see nothing in these preliminary results that vitiates the tsunami source that we posit in the next section.

A Plausible Tsunamigenic Source Location—the Semidi Subduction Sector: Rupture Dimensions and Geographic Placement

Our reasons for restricting the source area for the scenario tsunami to between the Shumagin Islands and Kodiak Island were given above. Thus, rupture length is limited to about 400 km or less. The regional depth limit for interplate thrust earthquakes on the Alaska Peninsula is about 45 km and the down-dip dimension of the Slab 1.0 plate boundary model from the Alaska Trench to that depth is about 200 to 220 km (Hayes and others, 2012). These are the spatial limits within which our scenario source must be placed. This requires a relatively compact source with a large average slip for a M_w~9 subduction earthquake. We show below that the source dimensions and moment magnitude of the 11 March 2011 Tohoku earthquake match these requirements and that there are many similarities in the geology and geophysics of these two subduction margins that make this application plausible.

Comparisons Between the Semidi and Tohoku Subduction Sectors

In table 2, we summarize the geologic and geophysical features in these two subduction-zone segments: relative plate motions, average age and sea-floor roughness of the incoming oceanic plate, average trench depths, forearc bathymetric morphologies, fault structures, average dip of the megathrust boundaries, the trench-to-shoreline distance, activities of the volcanic arcs, and other features. There is typically wide variability in these features among subduction zones of the world (Scholl and others, 2013). As discussed more fully by Ryan and others (2012a, 2012b), there are remarkable similarities in the seismic images of structures in the Tohoku and Semidi margins (fig. 4). The major differences, such as the ages of the incoming plates and trench sediment thicknesses, are not directly relevant to the question of tsunami potential, because the instrumental and historical record shows that great and giant subduction earthquakes occur over wide ranges of incoming plate ages and trench sediment fill (Scholl and others, 2013). Moreover, the basic structural similarities between these two subduction margins are obvious. One important feature of the Tohoku margin in the vicinity of the region of highest slip in 2011 is the presence of a large landward-dipping normal fault that was evidently reactivated during the 2011 earthquake (fig. 5). Japanese scientists have called this a branch fault because it branches off the megathrust boundary (Kodaira, 2012; Kodaira and others, 2012). This structure is thought to represent the dynamic adjustment of the offshore forearc to a steep gradient in coseismic slip on the subduction boundary. Such “branch” normal faults are seen in most seismic sections crossing the trench slope of the Alaska Peninsula (Bruns and others, 1987), but better resolution is needed to resolve such structures that cross the Semidi sector (fig. 4; Ryan and others, 2012b).

Characterizing the Scalar Seismic Moment of the 11 March 2011 Tohoku Earthquake, Slip Models, and Development of a Synoptic Slip Distribution Model and Target Range of Model Parameters

Because of the density of GPS, seismic, and tide-gage networks in Japan, sea-floor instruments offshore, and intense interest in using global tide-gage and seismic instruments, the 2011 Tohoku earthquake is the best-characterized subduction earthquake in history. The reported scalar seismic moments range from 3.8 to 5.7×10^{22} N·m, equivalent to an M_w of 9.0 to 9.1 (table 3), now among the five largest magnitudes in the instrumental record. We chose a scalar moment of 4.9×10^{22} N·m (M_w 9.1) as our target moment within this range of reported values. The Tohoku event has been extensively studied in the past 3 years. The resulting coseismic slip models vary greatly in the data that they use in their inversions, their methodologies, assumed subfault geometries, and other assumptions that went into these models. Naturally, there is a fairly wide diversity in the resulting models (table 4), including rupture lengths (160 to 440 km), down-dip dimensions (120 to 220 km), average slip (12 to 25 m), and peak coseismic slips (27 to 85 m). In general, those models constrained by local and regional Japanese data have the best spatial resolution from stations on land but have limited geographic coverage and resolution for slips on the subduction boundary near the Japan Trench far from land. On the other hand, those models that only use far-field tide-gage and seismic data have better geographic coverage but more limited spatial resolution. It was the measurements from sea-floor GPS, pressure gages, and tethered tsunami gages that supplied the most convincing evidence that unprecedented slip, as much as 85 m, occurred near the Japan Trench. Because most of these sea-floor instruments were located along a narrow trench-normal corridor, trench-parallel resolution was limited. In our opinion the most convincing models are the hybrid ones that incorporate far-field seismic and tide-gage data, onshore Japanese seismic, and onshore tide-gage data, as well as data from sea-floor instruments. Our expectation is that giant large-slip earthquakes like the 2011 Tohoku earthquake have occurred elsewhere in the past, but the lack of sea-floor data has prevented them from being identified. We posit that such an event could occur in the Semidi sector.

We abstract from such models the following simplified synoptic view of the 11 March 2011 source:

- A compact source with the following dimensions: 300 to 440 km long parallel to trench, and 150 to 200 km downdip
- Maximum coseismic slip near the trench: 65 m
- Average slip: ~18 m
- Bilateral rupture from the main-shock epicenter
- A rough along-strike symmetry, with peak slip along the trench segment midline and slip falloff toward the trench-parallel limits of rupture.

Creating a Subfault Grid and Applying a Tohoku-Type Slip Distribution to the Semidi Sector

A 3-D Megathrust Boundary Geometry and the Construction of Subfault Segments

We constructed an approximation of a curviplanar subfault geometry by the following procedure: Using geographic information system (GIS) tools, a first row of 25×50 km rectangular surface tiles was constructed with the southeast boundaries approximately coincident with a smoothed trench line and shared corners along this line. We then propagated this first row of tiles approximately perpendicular to the trench, producing an 8×8 array of surface tiles (fig. 6). Naturally, this array of tiles increasingly overlapped laterally with adjacent tiles interior to the array as new rows of tiles were created toward the volcanic arc. Those overlaps were graphically eliminated by creating shared lateral boundaries and corners (fig. 7). The trench-parallel subfault boundaries are approximately parallel to the lines representing depth contours in Slab 1.0 (fig. 2a). Finally, these polygonal surface tiles were projected vertically onto the Slab 1.0 surface and the resultant subfault areas adjusted as $A' = A/\cos\theta$ where A is the area of the surface tile, A' is the projected area of the plate-boundary subfault on the dipping plate boundary, and θ is the dip angle in the Slab 1.0 model at the centroid of the polygonal tile. Such a procedure produces subfaults of variable area, dip, and azimuths of line segments defining their boundaries and conforms to what we presently know about the 3-D geometry of this subduction sector.

Applying this Simplified Synoptic Slip Model for the 2011 Tohoku earthquake to the Semidi Sector Array

In adapting the foregoing abstraction from slip models of the Tohoku-Oki earthquake to the Semidi subduction sector, we imposed smoothly varying slip from subfault to subfault (figs. 8, 9, and 10). Abrupt changes in average slip distribution in subfaults are not considered justified and in any case should not affect the long-wavelength approximation of tsunami models in the far field. Seismic reflection surveys crossing the Japan Trench after the 2011 Tohoku earthquake show that trench-fill sediments and the outermost inner trench slope underwent distributed deformation by thrust faulting during the event (Kodaira and others, 2012). Accordingly, we expect that such distributed slip would represent an equivalent reduced maximum slip under the deformed soft sediments in the part of the Semidi frontal prism and trench-fill nearest the Aleutian Trench. The whole frontal prism in the Semidi sector is about 20 to 25 km wide, about the same width as in the Tohoku sector (von Huene and Cullota, 1989; von Huene and others 1994; Ryan and others, 2012b; von Huene and others, 2012).

The Final Version of the Semidi Sector Source

The lateral and down-dip dimensions of the final array are 358 km and 205 km, respectively, close to the targeted Tohoku-source dimensions (compare summary in the section above on developing model parameters for Tohoku and tables 4 and 5). The average dip of our Semidi array is about 12°, compared to the slightly larger average dip of the seismogenic megathrust boundary of about 13° for Tohoku (table 2). Using a depth-varying shear modulus of 30, 40, and 50 gigapascals (GPa), consistent with rock-physics models, the slip distribution that we adopted produces a summed seismic moment of 4.9×10^{22} N·m, which is close to the average value for the Tohoku-Oki source investigations summarized in table 3. The latitudes, longitudes, and depths at each corner of the subfault grid and at the subfault geometrical centroids are documented in the appendix (table A, Supplementary Information).

Scaling of Average Slip During Seismogenic Rupture for Giant Earthquakes with Moment Magnitude: How Useful a Guide is it?

Estimating source dimensions and moment magnitudes is difficult even in the digital era of seismology. Source dimensions estimated in the pre-digital era from aftershock distributions are suspect, in view of the fact that for recent giant subduction earthquakes, aftershocks extend far beyond the areas of significant modeled seismogenic slip. For example, the aftershock zone for the 2011 Tohoku earthquake is roughly twice as large as the coseismic area of significant slip (Hayes, 2011). Also, recent earthquakes of comparable moment magnitude—2004 Sumatra M_w 9.15 (Chlieh and others, 2007) and 2011 Tohoku M_w 9.1 (this synopsis)—have estimated average slips that differ by more than a factor of three to four (5 m versus 15 to 20 m, respectively). There is a similar scale of variability in average slip for smaller subduction earthquakes, although modeling of events smaller than M_w 8.0 becomes increasingly uncertain with decreasing moment magnitude. With such intrinsic variability, one can question the utility of using the scaling of average slip versus scalar seismic moment as a tool for forecasting possible earthquake ground motions and the tsunami wave field.

Satake and Tanioka (1996) and Satake and others (2008), in reviewing what was then known about large tsunamigenic subduction earthquakes worldwide, speculated about the role of poorly consolidated sediments in the outer forearc prism closest to the trench in seismogenesis and tsunamigenesis. For most big interplate thrust earthquakes, significant coseismic slip probably does not occur under the prism but does occur deeper in the megathrust boundary. For certain less frequent giant earthquakes, large slip can and does occur under the prism, often in conjunction with slip deeper along the subduction boundary. The Tohoku earthquake in 2011 was such a compound-rupture earthquake. Satake (2011), following the 2011 Tohoku event, proposed that such compound-rupture events may be a part of a “supercycle” of subduction earthquakes in some subduction zones that occur on millennial time scales and hence are distinct from more typical centuries-scale great subduction earthquake cycles that have smaller average slip. In a way, such segmentation is the downdip counterpart of the along-strike segmentation of ruptures that allows for infrequent multi-segment ruptures leading to great and giant supercycle tsunamigenic earthquakes, such as the *M* 8.4–8.6 Hoei earthquake of 28 October 1707 in the Nankai subduction zone (Ando, 1975). If such a view is correct, then the occurrence of supercycle earthquakes involving both up-dip/down-dip segmentation would lead to a different type of scaling than rupture just involving large but not exceptional slip down-dip of a forearc frontal prism. Our challenge is to search for geological and geophysical features of subduction zones that may give us insights into whether a particular subduction zone is prone to such supercycle subduction earthquakes.

Summary

Tsunami modeling has demonstrated that giant subduction earthquakes along the Pacific side of the Alaska Peninsula would produce more potent tsunami waves along California shorelines than would such earthquakes at any other distant location. GPS measurements indicate that the Semidi subduction sector between Kodiak Island and the Shumagin Islands is currently “locked” and has probably not experienced large seismogenic slip (>10 m) in centuries. In the search of a plausible coseismic slip source for a giant subduction earthquake in the critical Semidi sector of the Alaska subduction system, the USGS Tsunami Source Working Group for the SAFRR tsunami scenario used the source characteristics of the M_w~9 Tohoku earthquake as a proxy for a number of reasons:

- Close examination of the megathrust geometry, geology, and geophysics of the Semidi subduction sector off the Alaska Peninsula and the Tohoku margin off Japan indicates that, although not identical twins, these subduction systems share many features that are probably relevant factors in governing the occurrence of damaging far-field tsunami waves.
- The 2011 Tohoku earthquake is the best -characterized giant earthquake and tsunami source in history, and its occurrence has prompted a reevaluation of subduction systems elsewhere for the potential of similarly potent tsunami sources.
- The compact nature of the Tohoku source also makes it an ideal "fit" to the spatial dimensions of the Semidi subduction sector as we define it between Kodiak Island and the Shumagin Islands.
- When allowances are made for differences in methodologies, data used to constrain the models, and resolution limits, the parameters of our source model are consistent with the Tohoku model literature. We fitted a simple polygonal subfault array to the curviplanar shape of the plate boundary of the Semidi sector based on the USGS Slab 1.0 geometrical model for the sector. We then put forward a simplified synoptic slip distribution in this array to emulate the Tohoku earthquake based on our interpretations of the model literature for this event.
- The immense seismic moment of the Tohoku earthquake of 2011 was not anticipated, in spite of a long historical record of earthquakes in Japan. This fact underscores the importance of paleogeologic investigations along the Alaska subduction margin to establish a long-term prehistoric record of the occurrence of great and giant subduction earthquakes and the tsunami waves that they spawn.

References Cited

Abe, K., 1979, Size of great earthquakes of 1837–1974 inferred from tsunami data: Journal of Geophysical Research, v. 84, no. B4, p. 1561-1568, doi:10.1029/JB084iB04p01561.

Ando, M., 1975, Source mechanisms and tectonic significance of historical earthquakes along the Nankai trough: Tectonophysics, v. 27, no. 2., p. 119–140.

Bird, P., 2003, An updated digital model of plate boundaries: Geochemistry Geophysics Geosystems, v. 4, no. 3, p. 1027, doi:10.1029/2001GC000252.

Boyd, T. and Lerner-Lam, A.L.,1988, Spatial distribution of turn-of-the-century seismicity along the Alaska-Aleutian arc, Bull. Seismological Soc. Am. V. 78, p. 635-650.

Boyd, T.M., Taber, J.J., Lerner-Lam, A. L., and Beavan, J., 1988, Seismic rupture and arc segmentation within the Shumagin Islands Seismic Gap, Alaska: Geophysical Research Letters, v. 15, no. 3, p. 201-204.

Brockman, S.R., Espinosa, A.F., and Michael, J.A. 1988, Catalog of intensities and magnitudes for earthquakes in Alaska and the Aleutian lslands—I786–1981: U.S. Geological Survey Bulletin 1840, 199 p.
Bruns, T.R., von Huene, R., Culotta, R.C., Lewis, S.D., and Ladd, J.W., 1987. Geology and petroleum potential of the Shumagin margin, Alaska, chap. 8 *of* Scholl, D.W., Grantz, A. and Vedder, J.G., eds., Geology and resource potential of the continental margin of western North America and adjacent ocean basins—Beaufort Sea to Baja California: Houston, Tex., Circumpacific Council for Energy and Mineral Resources, Earth Science Series, v. 6, p. 157-189.
Carver, G.A., and Plafker, G., 2008, Paleoseismicity and neotectonics of the Aleutian subduction zone—an overview, *in* Freymueller, J.T., Haeussler, P.J., Wesson, R.L., and Ekström, G., eds., Active tectonics and seismic potential of Alaska: Washington D.C., American Geophysical Union, Geophysical Monograph Series, v. 179, p. 43-63.
Chlieh, M., and 10 others, 2007, Coseismic slip and afterslip of the great M_w 9.15 Sumatra–Andaman earthquake of 2004: Bulletin of the Seismological Society of America, v. 97, S152-S173, doi:10.1785/0120050631.
Christensen, D.H., and Beck, S.L., 1994, The rupture process and tectonic implications of the great 1964 Prince Williams Sound earthquake: Pageoph, v. 142, no. 1, p. 29-53.
Columbia University, 2013, Global Centroid Moment Tensor (CMT) Project: Last accessed February 2013. URL: http://www.globalcmt.org/
Cross, R.S., and Freymueller, J.T., 2008, Evidence for and implications of a Bering plate based on geodetic measurements from the Aleutians and western Alaska: Journal of Geophysical Research, v. 113, B07405, doi:10.1029/2007JB005136, 2008.
Davies, J., Sykes, L., House, L., and Jacob, K., 1981, Shumagin seismic gap, Alaska Peninsula; history of great earthquakes, tectonic setting, and evidence for high seismic potential: Journal of Geophysical Research, v. 86, p. 3821-3855.
Doser, D.I., 2006, Relocations of earthquakes (1899–1917) in south-central Alaska: Pure and Applied Geophysics, v. 163, p. 1461–1476.
Engdahl, E.R., and A. Villaseñor, 2002, Global Seismicity: 1900-1999, *in* W.H.K. Lee, H. Kanamori, P.C. Jennings, and C. Kisslinger, eds., International Handbook of Earthquake and Engineering Seismology*,* Part A, Chapter 41, pp. 665-690, Academic Press.
Estabrook, C.H., and Boyd, T.M., 1992, The Shumagin Islands, Alaska earthquake of 31 May 1917: Bulletin of the Seismological Society of America, v. 82, p. 755–773.
Estabrook, C.H., Jacob, K.H., and Sykes, L.R., 1994, Body wave and surface wave analysis of large and great earthquakes along the eastern Aleutian arc, 1923–1993: Implications for future events: Journal of Geophysical Research, v. 99, no. B6, p. 11643–11662.
Fletcher, H.J., Beavan, J., Freymueller, J., and Gilbert, L., 2001, High interseismic coupling of the Alaska subduction zone SW of Kodiak Island inferred from GPS data: Geophysical Research Letters, v. 28, no. 3, p. 443–446.
Fournier, T.J., and Freymueller, J.T., 2007, Transition from locked to creeping subduction in the Shumagin region, Alaska: Geophysical Research Letters, v. 34, L06303, doi:10.1029/2006GLO29073.

Freymueller, J.T., and Beavan, J., 1999, Absence of strain accumulation in the western Shumagin Segment of the Alaska subduction zone: Geophysical Research Letters, v. 26, no. 21, p. 3233–3336.
Freymueller, J.T., Woodard, H., Cohen, S.C., Cross, R., Elliott, J., Larsen, C.F., Hreinsdóttir, S., and Zweck, C., 2008, Active deformation in Alaska based on 15 years of GPS measurements, *in* Freymueller, J.T., Haeussler, P.J., Wesson, R.L., and Ekström, G., eds., Active tectonics and seismic potential of Alaska: Washington D.C., American Geophysical Union, Geophysical Monograph Series, v. 179, p. 1–42.
Fujii, Y., Satake, K., Sakai, S., Shinohara, M., and Kanazawa, T., 2011, Tsunami source of the 2011 off the Pacific coast of Tohoku earthquake: Earth Planets Space, v. 63, p. 815–820.
Haeussler, P.J., and Plafker, G., 1995, Earthquakes in Alaska: U.S. Geological Survey Open-File Report, 95-624, 1 sheet poster in pdf form.
Hayes, G., 2011, Rapid source characterization of the 2011 M_w 9.0 off the Pacific coast of Tohoku earthquake: Earth Planets Space, v. 63, p. 529–534.
Hayes, G.P., Wald, D.J., and Johnson, R.L., 2012, Slab 1.0: A three-dimensional model of global subduction zone geometries**:** Journal of Geophysical Research 117, B01302, doi:10.1029/2011JB008524.
Holdahl, S. and J. Sauber, 1993, Coseismic slip in the 1964 Prince William Sound earthquake: a new geodetic inversion, *Pageoph. ,* 14(4), 55-82.
Ichinose, G., Somerville, P., Thio, H.K., Graves, R., and O'Connell, D., 2007, Rupture process of the 1964 Prince William Sound, Alaska, earthquake from the combined inversion of seismic, tsunami, and geodetic data: Journal of Geophysical Research, v. 112, B07306, doi:10.1029/2006JB004728.
Ide, S., Baltay, A., and Beroza, G.C., 2011, Shallow dynamic overshoot and energetic deep rupture in the 2011 Mw 9.0 Tohoku-Oki earthquake: Science, v. 332, p. 1426–1429, doi:10.1126/science.1207020.
Iinuma, T., and 11 others, 2011, Coseismic slip distribution of the 2011 off the Pacific Coast of Tohoku earthquake deduced from land and seafloor geodesy: Abstract G51A-0853, presented at 2011 Fall Meeting, American Geophysical Union, San Francisco, California, 5–9 December.
Iinuma, T., and 10 others, 2012, Coseismic slip distribution of the 2011 off the Pacific Coast of Tohoku Earthquake (M9.0) refined by means of seafloor geodetic data: Journal of Geophysical Research 117, B07409, 18 p., doi:10.1029/2012JB009186.
International Seismological Center, 2013, ISC-GEM Global Instrumental Earthquake Catalogue (1900-2009): Accessed [February 2013] at http://www.isc.ac.uk/iscgem/.
Ito, Y., Tsuji, T., Osada, Y., Kido, M., Inazu, D., Hayashi, Y., Tsushima, H., Hino, R., and Fujimoto, H., 2011, Frontal wedge deformation near the source region of the 2011 Tohoku-Oki earthquake: Geophysical Research Letters, v. 38, no. 7, L00G05, doi:10.1029/2011GL048355.
Johnson, J.M., and Satake, K, 1994, Rupture extent of the 1938 Alaskan earthquake as inferred from tsunami waveforms: Geophysical Research Letters. v. 21, p. 733, doi:10.1029/94GL00333.
Johnson, J. M., and K. Satake, 1995, Source parameters of the 1957 Aleutian and 1938 Alaskan earthquakes from tsunami waveforms, in: "Tsunami: progress in prediction, disaster prevention and warning", eds. Y. Tsuchiya and N. Shuto, p. 71-84, Kluwer.

Johnson, J.M. and Satake, K., 1997, Estimation of seismic moment and slip distribution of the April 1, 1946, Aleutian tsunami earthquake: Journal of Geophysical Research, v. 102, p. 11765–11774.

Johnson, J.M., Satake, K., Holdahl, S.R., and Sauber, J., 1996, The 1964 Prince William Sound earthquake; joint inversions of tsunami and geodetic data: Journal Of Geophysical Research, v. 101, p. 523–532.

Kanamori, H., 1972, Mechanism of tsunami earthquakes: Physics of Earth and Planetary Interiors, v. 6, p. 346–359.

Kodaira, S., 2012, Marine geophysical survey of Tohoku quake rupture zone (abs.): Network for Earthquake Engineering Simulation, last accessed in February 2013. URL at http://nees.org/resources/4176.

Kodaira, S., No, T., Nakamura, Y., Fuiwara, T., Kaiho, Y., Miura, S., Takahashi, N., Kaneda, Y., and Taira, A., 2012, Coseismic fault rupture at the trench axis during the 2011 Tohoku-oki earthquake: Nature Geoscience, v. 5, p. 646–650, doi:10.1038/ngeo1547.

Koketsu, K., Yokota, Y., Nishimura, N., Yagi, Y., Miyazaki, S., Satake, K., Fujii, Y., Miyake, H., Sakai, S., Yamanaka, Y., and Okada, T., 2011, A unified source model for the 2011 Tohoku earthquake: Earth and Planetary Science Letters, v. 310, p. 480–487.

Lander, J.F., 1996, Tsunamis affecting Alaska 1737-1996: Boulder, Colorado, National Oceanic and Atmospheric Administration, National Geophysical Data Center, 155 p. Available online at http://www.ngdc.noaa.gov/hazard/data/publications/Kgrd-31.pdf.

Lander, J.F., and Lockridge, P.A., 1989, United States tsunamis (including United States possessions) 1690–1988: Boulder, Colorado, National Oceanic and Atmospheric Administration, National Geophysical Data Center, Publication 41-2., http://www.ngdc.noaa.gov/seg/hazard/data/tsupub/pub41-2.pdf.

Lay, T., Ammon, C.J., Kanamori, H., Xue, L., and Kim, M.J., 2011, Possible large near-trench slip during the 2011 Mw 9.0 off the Pacific coast of Tohoku earthquake: Earth Planets Space, v. 63, no. 7, p. 687–692.

Lopéz, A., and Okal, E.A., 2006, A seismological reassessment of the source of the 1946 Aleutian 'tsunami' earthquake: Geophysical Journal International, v. 165, p. 835–849.

McCaffrey, R., 2007, The Next Great Earthquake, Science, v. 315, p. 1675-1676.

McCaffrey, R., 2008, Global frequency of magnitude 9 earthquakes, Geology, 36, 263-266.

Minson, S.E., Simons, M., Beck, J.L., Jiang, J., Ortega Culaciati, F.H., Inbal, A., Owen, S.E., and Sladen, A., 2011, A Bayesian exploration of kinematic rupture parameters for the great 2011 Tohoku-Oki earthquake: American Geophysical Union, Fall Meeting 2011, abstract U41D-06.

Minoura and 5 others, 2001, The 869 Jogan tsunami deposit and recurrence interval for large-scale tsunami on the Pacific coast of northeast Japan, Journal of Natural Disaster Science, v. 23, p. 83-88.

Nettles, M., Ekström, G., and Koss, H., 2011, Centroid-moment-tensor analysis of the 2011 off the Pacific coast of Tohoku earthquake and its larger foreshocks and aftershocks: Earth Planets Space, v. 63, p. 519–523.

National Geophysical Data Center, 2012, Global tsunami events and runups: National Oceanic and Atmospheric Administration, National Geophysical Data Center, last accessed January 2012, at http://www.ngdc.noaa.gov/hazard/tsu_db.shtml.

Novosibirsk Tsunami Laboratory, 2012, Historical tsunami database for the world ocean: Accessed February, 2012 at http://tsun.sscc.ru/nh/tsunami.php.
Okal, E.A., Synolakis, C.E., Fryer, G.J., Heinrich, P., Borrero, J.C., Ruscher, C., Arcas, D., Guille, G., and Rousseau, D., 2002, A field survey of the 1946 Aleutian tsunami in the far field: Seismological Research Letters, v. 73, p. 490–503.
Okal, E.A., Plafker, G., Synolakis, C.E., and Borrero, J.C., 2003, Near-field survey of the 1946 Aleutian tsunami on Unimak and Sanak Islands: Bull. Seismological Society of America, v. 93, p. 1226–1234.
Ozawa, S., Nishimura, T., Suito, H., Kobayashi, T., Tobita, M., and Imakiira, T., 2011, Coseismic and postseismic slip of the 2011 magnitude-9 Tohoku-Oki earthquake: Nature, v. 475, p. 373–376.
Pacheco, J., and Sykes, L.R., 1992, Seismic moment catalogue of large shallow earthquakes, 1900 to 1989: Bulletin of the Seismological Society of America, v. 82, p. 1306–1349.
Pararas-Carayannis, G., and Calebaugh, P.J., 1977, Catalog of tsunamis in Hawaii, revised and updated: National Oceanic and Atmospheric Administration, World Data Center A for Solid Earth Geophysics, 78 p.
Pollitz, F., Bürgmann, R., and Banerjee, P., 2011, Geodetic slip model of the 2011 M9.0 Tohoku earthquake: Geophysical Research Letters, v. 38, L00G08, doi:10.1029/2011GL048632
Ryan, H.F., von Huene, R., Scholl, D., and Kirby, S., 2012a, Tsunami hazards to U.S. coasts from giant earthquakes in Alaska: Eos (American Geophysical Union Transactions), v. 93, p. 185–186.
Ryan, H.F., von Huene, R., Wells, R. E., Scholl, D. W., Kirby, S., and Draut, A. E., 2012b, History of earthquakes and tsunamis along the eastern Aleutian-Alaska Megathrust, with implications for tsunami hazards in the California Continental Borderland: U.S. Geological Survey Professional Paper 1795–A, 31 p.
Santini, S., Dragoni, M., and Spada, G., 2003, Asperity distribution of the 1964 Great Alaska earthquake and its relation to subsequent seismicity in the region: Tectonophysics, v. 367, p. 219–233.
Satake, K., 2011,The great off Tohoku earthquake of 11 March 2011: Presentation at International Union of Geodesy and Geophysics Meeting, Melbourne, Australia, 28 June – 7 July 2011.
Satake, K. and Tanioka, T., 1996, Source of tsunami and tsunamigenic earthquakes in subduction zones, Pure and Appl. Geophysics, v. 94, p. 467–483
Satake, K., and Tanioka, Y., 1999, Sources of tsunami and tsunamigenic earthquakes in subduction zones: Pure and Applied Geophysics, v. 154, p. 467–483.
Satake, K., Sawai, Y., Shishikura, M., Okamura, Y., Namegaya, Y., and Yamaki, S., 2007, Tsunami source of the unusual AD 869 earthquake off Miyagi, Japan, inferred from tsunami deposits and numerical simulation of inundation: American Geophysical Union, Fall Meeting 2007, Abstract #T31G-03.
Satake, K., Namegaya, Y., and Yamaki, S., 2008, Numerical simulation of the AD 869 Jogan tsunami in Ishinomaki and Sendai plains: Geological Survey of Japan, Active Fault and Earthquake Center, Report no. 8, p. 71–89. Available online at http://unit.aist.go.jp/actfault-eq/seika/h19seika/pdf/03.satake.pdf.

Scholl, D.W., Kirby, S.H, von Huene, R., Ryan, H., and Wells, R.W., 2013, Great megathrust earthquakes and the subduction of thick sections of sediment, tectonically eroded debris, and low-relief sea floor, *in* Fildani, A., Piper, D.J.W., and Scholl, D., eds., Exploring the deep sea and beyond—contributions to marine geology in honor of William R. Normark: Geological Society of America, Geosphere, in press.

Shao, G., and Ji, C., 2011, Rupture characterizations of the 2011 Mw 9.1 off the Pacific coast of Tohoku earthquake and its March 9th Mw 7.4 foreshock constrained by an unprecedented dataset for subduction earthquakes: American Geophysical Union, Fall Meeting 2011, abstract U34A-03.

Shao, G., Li, X., Ji, C., and Maeda, T., 2011, Focal mechanism and slip history of the 2011 M_w 9.1 off the Pacific coast of Tohoku earthquake, constrained with teleseismic body and surface waves: Earth Planets Space, v. 63, p. 559–564.

Shillington, D.J., Bécal, A., Nedimovich, M.R., Kuhn, H., and Webb, S.C., 2012, Along-strike variations in the structure of the downgoing plate in the subduction zone off the Alaska Peninsula: American Geophysical Union, Fall Meeting 2012, abstract T13H-02

Siebert, L., Simkin, T., and Kimberly, P., 2011, Volcanoes of the world (3d ed.): Smithsonian Institution and University of California Press, 551 p.

Simons, M., and 14 others, 2011, The 2011 magnitude 9.0 Tohoku-Oki earthquake; mosaicking the megathrust from seconds to centuries: Science, v. 322, p. 1421–1425, doi:10.1126/science.1206731, 2011.

Smithsonian National Museum of Natural History, 2013, Global volcanism program; volcanoes of the world: Last accessed in February 2013 at http://www.volcano.si.edu/index.cfm.

Soloviev, S.L., 1968, The Sanak Kodiak Island tsunami of 1788 [in Russian]: Moscow, Nauka, The Tsunami Problem, Moscow, Nauka, p. 232–237. [English translation in Science of Tsunami Hazards, v. 8, no. 1, p. 34-38, 1990.]

Soloviev, S.L., and Go, Ch.N., 1975, Catalogue of tsunamis on the eastern shore of the Pacific Ocean [in Russian]: Moscow, Nauka, 203 p. [Translated into English by the Canadian Institute for Scientific and Technical Information, National Research Council, Ottawa, Canada.]

Sugawara, D., 2011, Deposits of the 869 Jogan and 2011 Tohoku-oki tsunamis: Unpublished Field Guide and Supplement (26 October field trip to near-coastal sites along Sendai Bay south of Sendai).

Sugawara, D., Imamura, F., Goto, K., Matsumoto, H., and Minoura, K., 2011, The 869 Jogan and the 2011 Tohoku-oki earthquake tsunamis: American Geophysical Union, Fall Meeting 2011, Abstract NH13G-08.

Suito, H., and Freymueller, J.T., 2009, A viscoeleastic and afterslip postseismic deformation model for the 1964 Alaska earthquake: Journal of Geophysical Research, v. 114, no. B11, doi:10.1029/2008JB005954.

Sykes, L.R., 1971, Aftershock zones of great earthquakes, seismicity gaps, and earthquake prediction for Alaska and the Aleutians: Journal of Geophysical Research, v. 76, p. 8021–8041.

Sykes, L.R., Kissinger, J.B., House, L., Davies, J.N., and Jakob, K.H., 1981, Rupture zones of great earthquakes in the Alaska-Aleutian Arc, 1784 to 1980: Journal of Geophysical Research, v. 86, p. 3821–3855.

Thio, H.K., Somerville, P., and Polet, J., 2010, Probabilistic tsunami hazard in California: Pacific Earthquake Engineering Research Center, PEER_ Report 2010–108, 61 p. Available online at http://peer.berkeley.edu/publications/peer_reports.html.

von Huene, R., and Culotta, R., 1989, Tectonic erosion at the front of the Japan Trench convergent margin: Tectonophysics, v. 160, p. 75–90.

von Huene , R., Klaeschena, D., Cropp, B., and Miller, J., 1994, Tectonic structure across the accretionary and erosional parts of the Japan Trench margin: Journal of Geophysical Research, v. 99, p. 22349–22361.

von Huene, R., Miller, J., and Weinrebe, W., 2012, Subducting plate geology in three great earthquake ruptures on the western Alaska margin, Kodiak to Unimak: Geosphere, v. 8, no. 3, p. 628–644, doi:10.1130/GES00715.

Wells, R.E., Blakely, R.J., Scholl, D.W., and Dinterman, P.A., 2003, Basin-centered asperities in great subduction zone earthquakes—a link between slip, subsidence, and subduction erosion?: Journal of Geophysical Research, v. 108, p. 2507, doi:10.1029/2002JB002072.

Wells, R.E., Blakely, R.J., Scholl, D.W., and Ryan, H.F., 2011, Seismicity, topography, and free-air gravity of the Aleutian-Alaska subduction zone: American Geophysical Union, Fall Meeting 2011, abstract T21B-2322.

Wesson, R.L., Boyd, O.S., Mueller, C.S., Bufe, C.G., Frankel, A.D., and Petersen, M.D., 2007, Revision of time-independent probabilistic seismic hazard maps for Alaska: U.S. Geological Survey Open-File Report 2007–1043, 33 p.

Witter, R.C., Engelhart, S.E., Briggs, R.W., Koeler, R.D., and Gelfenbaum, G., 2012, Little strain accumulation and release on the Alaska-Aleutian megathrust beneath the Shumagin Islands in the last 3400 Years?: Geological Society of America Abstracts with Programs, v. 44, no. 7, p. 413, https://gsa.confex.com/gsa/2012AM/webprogram/Paper206745.html.

Yagi, Y., and Fukuhata, Y., 2011, Rupture process of the 2011 Tohoku-oki earthquake and absolute elastic strain release: Geophysical Research Letters, v. 38, no. L19307, doi:10.1029/2011GL048701.

`

Table 1. Large instrumentally documented earthquakes and tsunami runups in the Semidi Sector and adjacent sectors of the Aleutian-Alaska subduction zone.

[Dates given as year (YYYY), month (MM), day (DD), hour (hh), minute (mm), and second (ss.s); epicenters for events before 1920 generally have large uncertainties; NR, no tsunami runups or damage reports at this site for this event in online tsunami databases of the National Geophysical Data Center (NGDC) and the Novosibirsk Tsunami Laboratory; X, no records or no instruments known to be in operation; s, shallow (<60 km), presumed or established; - , no data]

YYYY	MM	DD	HH	MM	SS.S	Tsunami reports?	Latitude °N	Longitude °E	Depth, km	M_w/M_s	Max. tsunami runup, m									
											San Diego, CA	Long Beach, CA	Los Angeles, CA	Santa Monica, CA	Half Moon Bay, CA	Cres-cent City, CA	Seward. AK	Hilo Harbor, HI	Largest far-field wave height	Largest near-field wave height
1938[1]	11	10	20	18	41.2	Yes	55.18	-158.181	25	8.2-8.3	0.1	X	NR	0.05	NR	0.18	0.08	0.3	0.3	0.1
1948[2]	5	14	22	31	43.4	No	54.71	-160.880	s	7.2	X	X	X	X	X	X	X	X	-	-
1989[3]	9	4	13	15	0.2	No	55.63	-156.912	s	7.0	NR	NR	NR	NR	NR	NR	NR	NR	-	-
1906[4]	12	23	17	22	0.0	No	56.85	-153.900	s	7.2	X	X	X	X	X	X	X	X	-	-
1917[5]	5	31	8	47	20.0	No	54.93	-159.433	29	7.4	X	X	X	X	X	X	X	X	-	-
1917[6]	12	21	17	54		No	55.29	-152.350	s	7.3	X	X	X	X	X	X	X	X	-	-
1917[7]	12	28	21	14		No	55.59	-152.750	s	>7	X	X	X	X	X	X	X	X	-	-
1946[8]	4	1	12	29	1.6	Yes	53.31	-162.880	s	8.6	0.2	0.2	0.34	X	3.5	0.9	0.1	8.8	20	42.0
1964[9]	3	28	3	36		yes	61.04	-147.730	s	9.2 to 9.3	0.5	NR	0.49	1.08	3.8	4.79	NR	3.0	4.8	34.4

1. No reported runups in AK exceeding 0.1 m. Tsunami modeling suggests three small slip patches averaging ~ 1.1 m [Johnson and Satake, 1994, 1995]. Average slip ~2 m based on seismic waveform modeling (Estabrook and others.,1994). This weak tsunami source only had 9 sites reporting, probably all tide gauge stations; **2.** Location: Sykes (1971). M_w: Estabrook and others (1994). No known tsunami observations (Not in NGDC tsunami source database); **3.** M_w (Harvard and Global CMT. Location; **4.** Epicenter: Doser (2006); Ms: Pacheco and Sykes (1992); No known tsunami observations (Not in NGDC tsunami source database); **5.** Epicenter: Boyd & Lerner-Lam 1988). $M_w = M_s$ from Estabrook and Boyd, (1992). No known tsunami observations (Not in NGDC tsunami source database); **6.** Doser (2006)*. Possible off trench location. No known tsunami observations (Not in NGDC tsunami source database); **7.** Diane Doser (2006)*. Possible off-trench location. No known tsunami observations (Not in NGDC tsunami source database); **8.** Epicenter and M_w: Lopez and Okal (2006); Epicenter near trench. Slow rupture. Far-field runup survey (Okal et al., 2003)/ Near-field survey (Okal et al., 2002). NGDC lists 508 tsunami record sites. Okal and others (2003) adds another 54.; **9.** Two patches of slip, one under Prince William Sound, another trenchward of Kodiak Island. NGDC lists 391 tsunami record sites.

Table 2. Geological and geophysical comparisons between the Semidi Sector of the Aleutian-Alaska subduction zone and the Tohoku Sector of the Japan-Trench subduction zone.

[mm/y, millimeters per year; Ma, millions of years ago; m, meters; km, kilometers; *M,* magnitude]

Feature	Semidi Sector, Alaska	Tohoku Sector, Japan	Sources and Notes
Convergence rate , mm/y	60 (nearly trench-normal motion). Pacific: Alaska peninsula relative motion.	83 (nearly trench-normal motion). Pacific Plate: Okotsk Plate relative plate motion.	Bird, 2003; Freymueller and others, 2008, Cross and Freymueller (2008). Both moderately fast rates.
Age of incoming plate, Ma	48-58	120-140	*M* 8.5 to 9.5 strongly tsunamigenic events (instrumental and historical) show no apparent trend with incoming plate age, ranging from 10 (Cascadia) to 140 (Tohoku) Ma for such subduction sectors.
Sea-floor roughness of trench fill bathymetery on incoming plate	Relatively smooth (Fig. 2A) with some local trench sea-floor roughness partly muted by sediment fill.	Smooth except near Japan Trench cusps and ~500 m normal fault scarps offsetting sediment (Fig. 2B)	Smooth incoming sea-floor is often associated with M_w >8.7 earthquakes with long rupture runouts, presumably caused by fewer geometrical barriers to rupture (Scholl and others, 2013).
Thickness of trench fill, m	1.25 km [Shillington and others (2012)]	0.5 km (von Huene and others, 1994)	Ryan, H. and Draut, A., 2012, unpublished map showing sediment fill in the Aleutian trench.

Feature	Semidi Sector, Alaska	Tohoku Sector, Japan	Sources and Notes
Thickness of subduction channel sediments landward of frontal prism, km	~1.0 ± 0.5	~1.0 ± 0.5	Ryan and others, 2012
Average trench depth, km	5	7	Depends on trench sedimentary fill.
Maximum throws of off- trench normal faults, m	>250 m (Shillington and others, 2012). Scarps only cut abyssal sediments.	~500 m (Japan Coast Guard website). Scarps only cut abyssal sediments.	Scarps probably not strong barriers to interplate thrust faulting since only sediments need be deformed.
Off-trench seismicity and outer-rise expression: seismicity rate and maximum magnitude	Rate: Low except south and southwest of Kodiak; Maximum magnitude: ~ 7	Rate: High; Maximum magnitude: 8.6	Differences in off-trench seismicity rates reflect differences in plate age and thickness. Doser (2006) relocated several large off-trench and near-trench events that occurrred in 1917 south of Kodiak Island, possibly in the Pacific Plate (See Table I).
Approximate regional depth limit of interplate thrust earthquakes offshore of Alaska Peninsula SW of Kodiak Island.	~55	~50	Slab 1.0 model (Hayes and others, 2012)
Average trench fill, km	1.5 ± 0.5	0.75 ± 0.5	Von Huene and others, 1994), Holly Ryan (personal communication, 2012)
Forearc bathymetric features	Trench-parallel ridges in frontal prism	Trench-parallel ridges in frontal prism	
	Prominent ridge near transition between frontal prism and slope basins	Muted ridge	
	Forearc sedimentary basins	Forearc sedimentary basins	

Feature	Semidi Sector, Alaska	Tohoku Sector, Japan	Sources and Notes
Offshore forearc structure and tectonics	*Frontal Prism and Transition*: Thrust faults & folds extending into trench sediment fill. Downdip prism width: ~25 km .	*Outer Prism and Transition*: Thrust faults & folds extending into trench sediment fill. Down-dip prism width ~20 km.	Ryan and others (2012); Roland von Huene, unpublished data 2012.
	Transition zone: Possible branch normal faults and thrust faults	*Transition* zone: Branch normal faults and thrust faults	Ryan and others (2012)
	Shelf: Shumagin Basin revealed by bathymetry, seismic reflection and gravity lows and basin-bounding gravity gradients.	*Shelf*: Discontinuous basins revealed by seismic reflection and gravity lows and basin-bounding gravity gradients.	Bruns and others (1987); Wells and others (2003), Wells and others (2011), Ryan and others (2012)
	High-wave-speed "basement" rocks extend to within about 20-30 km of the Alaska trench.	*High-wave-speed "basement" rocks* extend to within about 20-30 km of the Japan trench.	Ryan and others (2012)
Average seaward forearc plate boundary dip and (dip range in 10 km depth segments to ~50 km depth).	12° (5 to 20°)	13° (5 to 23°)	Determined from Slab 1.0 model (Hayes and others, 2012)
Average trench-to-shoreline distance, km	~240	~220	Measured using Google Earth. Only appoximate given complex coastlines.
Average trench to volcanic arc distance, km	~290	~290	Measured using Google Earth
Volcanic arc activity	Vigorous arc including Holocene caldera-forming eruptions	Vigorous arc including Holocene caldera-forming eruptions	Siebert, Simkin, and Kimberly (2011), Volcanoes of the World.

Table 3. Estimates of the seismic moment and moment magnitude of the 11 March 2011 Tohoku earthquake.

[CMT, Centroid Moment Tensor Project ; USGS, U.S. Geological Survey]

Reference	Method	Moment, N-m*10^{22}	M_w
Global CMT	CMT	5.30	9.1
USGS	CMT	4.5	9.0
Hayes (2011)	Teleseismic waveform inversion	4.04	9.0
USGS website	W phase inversion	3.9	9.0
UCSB (Shao and Ji (2011), fall 2011 AGU Abstract and presentation	Seismic: teleseismic waveform inversion, strong motion, GPS (land and sea-floor)	5.36	9.1
Lay and others (EPS 2011) P-MOD2 model and fall 2011 AGU presentation	Teleseismic P-wave waveform modeling	3.84	9.0
Yagi and Fukuhata (2011)	Teleseismic waveform inversion	5.7	9.1

Table 4. Models of slip distribution for the M_w 9.1 Tohoku earthquake.

[L, lengh of rupture; W, width of rupture; km, kilometers; Av., average; m, meters; PG, pressure gage; GPS, Global Positioning System; TG, tide gage; Wfs, waveforms; SM, strong motion; BB, broadband; *, circumscribed by resolution limits]

Reference	Data types	L, km	W, km	Av. slip, m	Min. Slip, m	Max. slip, m
Ito and others (2011)	Sea-floor PG GPS					80
Iinuma and others (2012)	Sea-floor PG, GPS,tide and tsunami gages	160*	120*	~20	0	85
Fujii and others (2011)	Tsunami model	350	200	~20	2	40
Ozawa and others (2011)	Japan GPS	400	~200	~12	4	27
Pollitz and others (2011)	Japan and regional GPS, sea-floor GPS	440	180	12-16	~5	~35
Shao and Ji (2011); Shao and others (2011)	Broadband wave-forms, GPS, TG	330	180	25	4	70
Minson and others (2011); Simons and others (2011)	Regional GPS teleseismic/tsunamic Wfs, GPS	160*	120*	20-25	~10	65
Koketsu and others (2011)	Teleseismic Wfs, SM, GPS, tsunami observations	310	180	~18	~5	~40
Lay and others (2011)	BB P-waveforms	320	220	15.9	4	62
Ide and others (2011)	Teleseismic Wfs	330	220	~15	0	30
Hayes (2011)	Teleseismic Wfs	~300	150	~15	~4	32
Yagi and Fukuhata (2011)	Teleseismic Wfs	~350	175	~20	~5	50

Table 5. Summary table of properties for the Semidi Sector coseismic slip model.

Property Name	Value	Minimum	Maximum
Number of subfaults	64		
Total source length, L at trench, km	358		
Range of summed subfault lengths along row, km		322	358
Total source downdip width, W, km	205		
Total area of subfaults, km^2	73,396		
Average subfault area, km^2	1147		
Range of subfault areas, low/high, km^2		1,056	1,242
Average slip, m	18.6		
Slip range, low/high, m	0	65	
Total seismic moment, Mo, N·m	4.91×10^{22}		
Moment magnitude, M_w	9.13		
Epicenter: latitude (°N) (d4 Centroid)[1]	55.8		
Epicenter: longitude (°E) (d4 Centroid)[1]	-156.7		

[1] The centroid of an epicenter is the location of the weighted average of the earthquake slip.

Figures

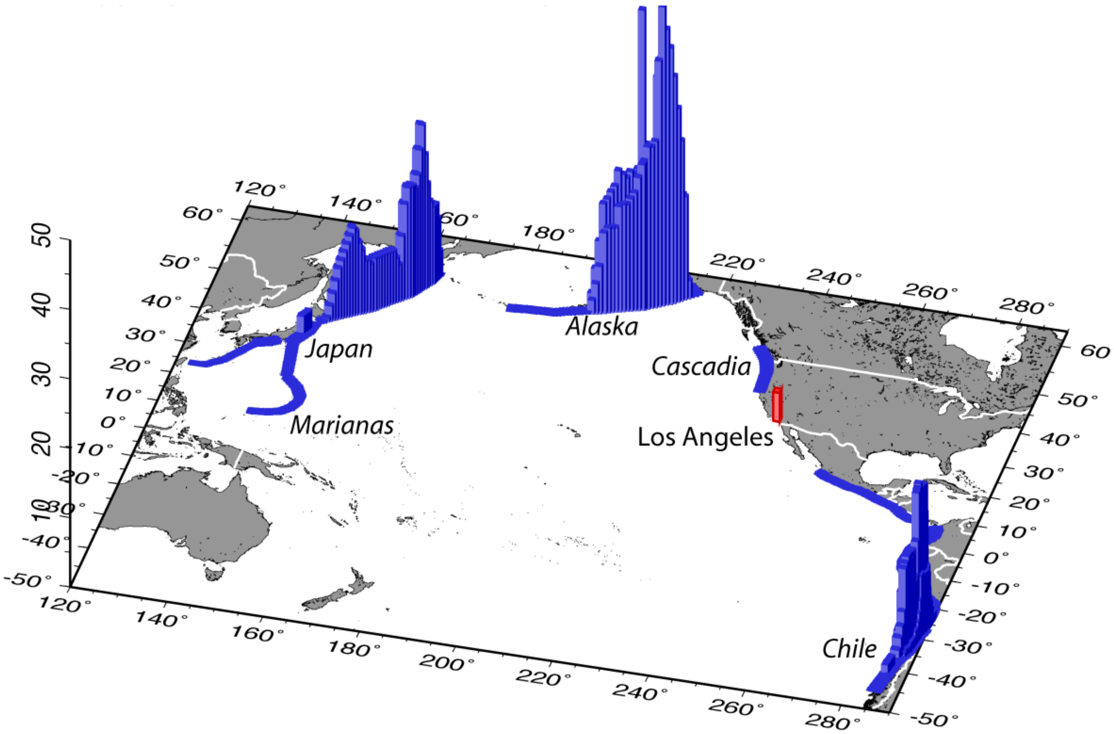

Figure 1. Map of the Pacific region showing source disaggregation for Los Angeles for tsunami peak wave height at 475-year return period (courtesy of Hong Kie Thio, URS Corporation). Vertical bar heights show that subduction earthquakes along the Alaska Peninsula have the greatest impacts on Los Angeles shorelines for a give seismic moment of the source subduction earthquake.

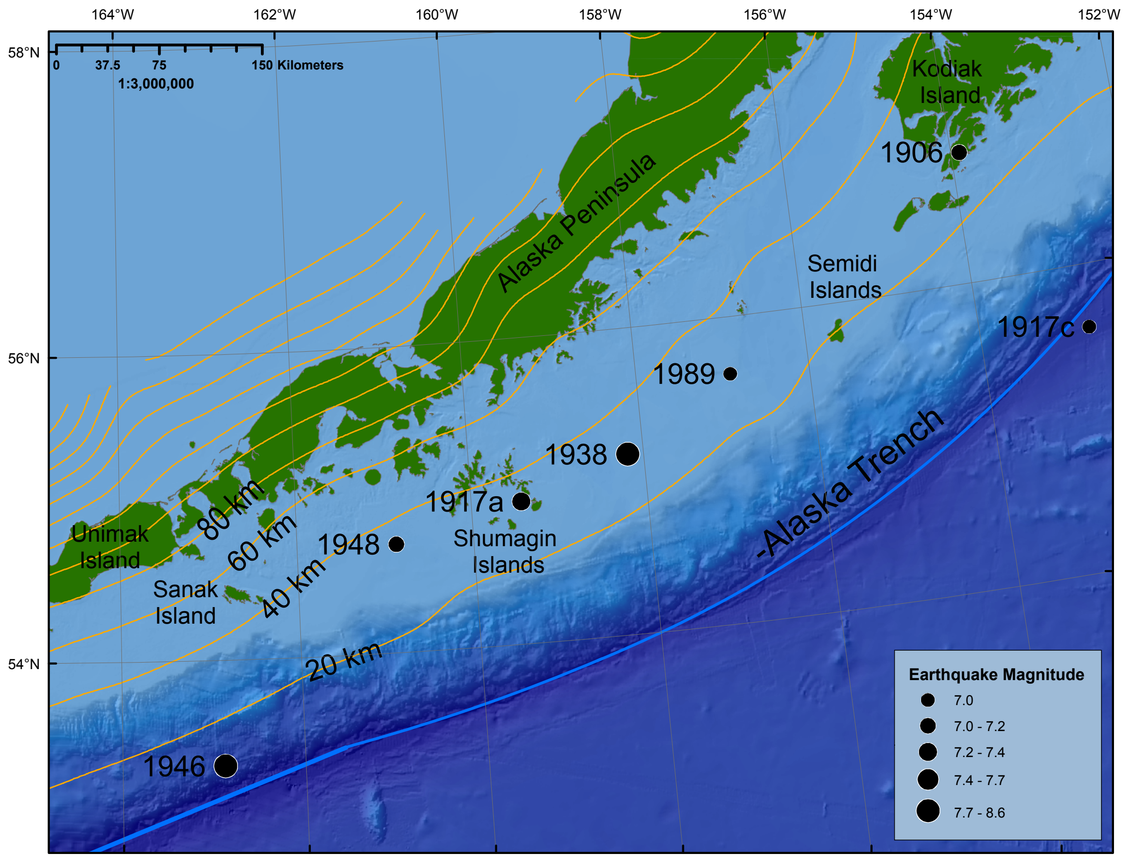
164°W
162°W
160°W
158°W
156°W
154°W
152°W
58°N
56°N
54°N
0 37.5 75 150 Kilometers
1:3,000,000
Kodiak Island
1906
Alaska Peninsula
Semidi Islands
1917c
1989
1938
1917a
1948
Shumagin Islands
Unimak Island
Sanak Island
80 km
60 km
40 km
20 km
Alaska Trench
1946
Earthquake Magnitude
7.0
7.0 - 7.2
7.2 - 7.4
7.4 - 7.7
7.7 - 8.6

Figure 2A

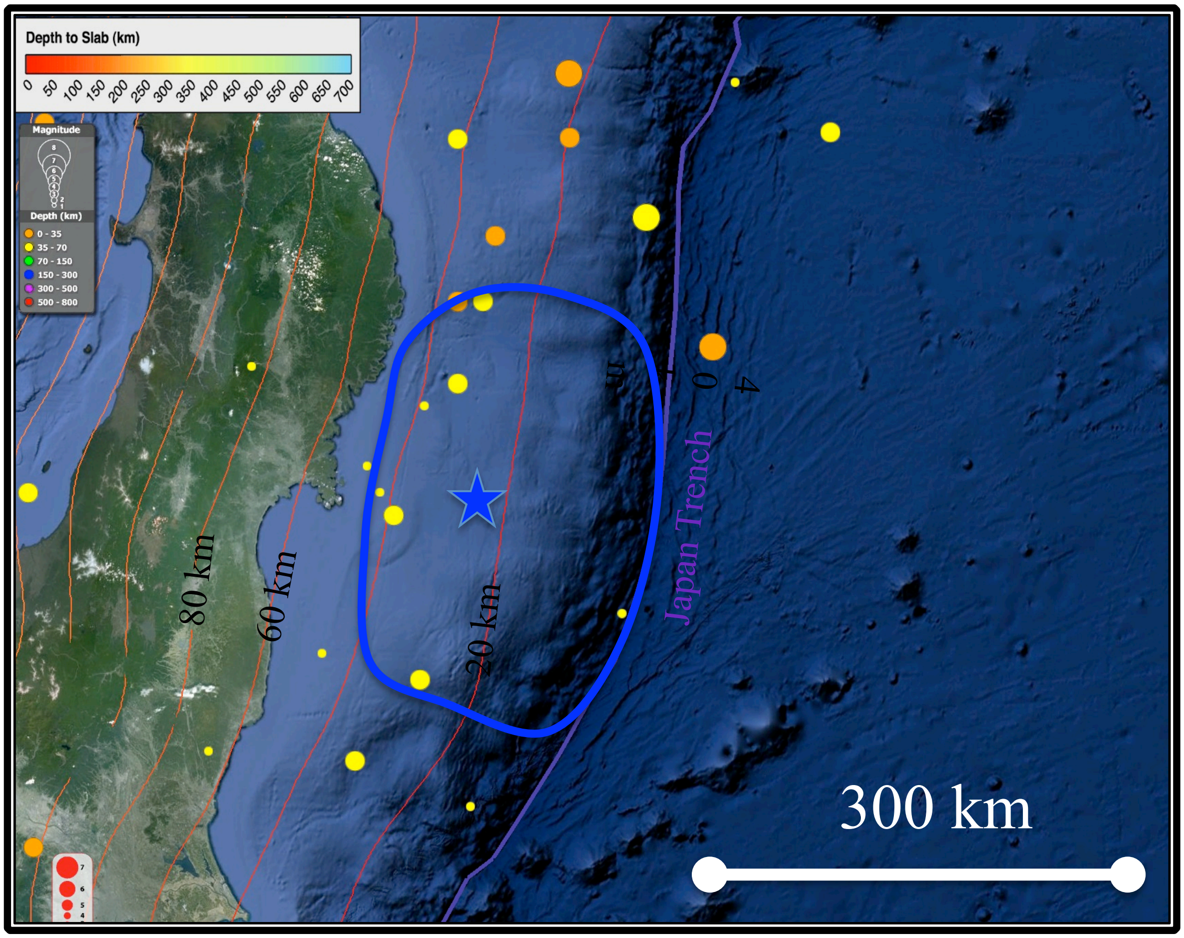

Figure 2. Maps showing locations of large earthquakes along the Aleutian-Alaska and the Tohoku, Japan, subduction margins. *A*, Summary map of the locations of large (Mw ≥ 7.0) shallow (<60 km) earthquakes along the southwest end of the Alaska Peninsula subduction sector since 1900 (filled black symbols are the epicenters of presumed interplate thrust earthquakes that have occurred since 1900). The yellow contours represent 20-km depth intervals from the Slab 1.0 model (Hayes and others, 2012), and the blue line is the axis of the Alaska-Aleutian trench at an average water depth of about 5 km. Earthquake data sources: Sykes (1971), Boyd and others (1988), Estabrook and others (1994), Engdahl and Villaseñor (2002), Doser (2006), ISC-GEM catalogue of earthquake magnitudes (2012). *B*, Summary map of the locations of large (Mw ≥ 7.0) shallow (<60 km) earthquakes along the Japan Trench subduction sector that occurred since 1900 and before 2011 (filled orange and yellow symbols are the epicenters of presumed interplate thrust earthquakes). The epicenter and approximate area of significant rupture for the M9.1 Tohoku earthquake of 11 March 2011 are shown as a blue star and a blue closed line segment, respectively. The rupture area overlaps the epicentral areas of numerous M≥7.0 earthquakes. Note that the majority of the epicenters of large events occurred at depths between 20 and 40 km, as is the case for the Semidi sector of the Alaska Peninsula (shown in a).

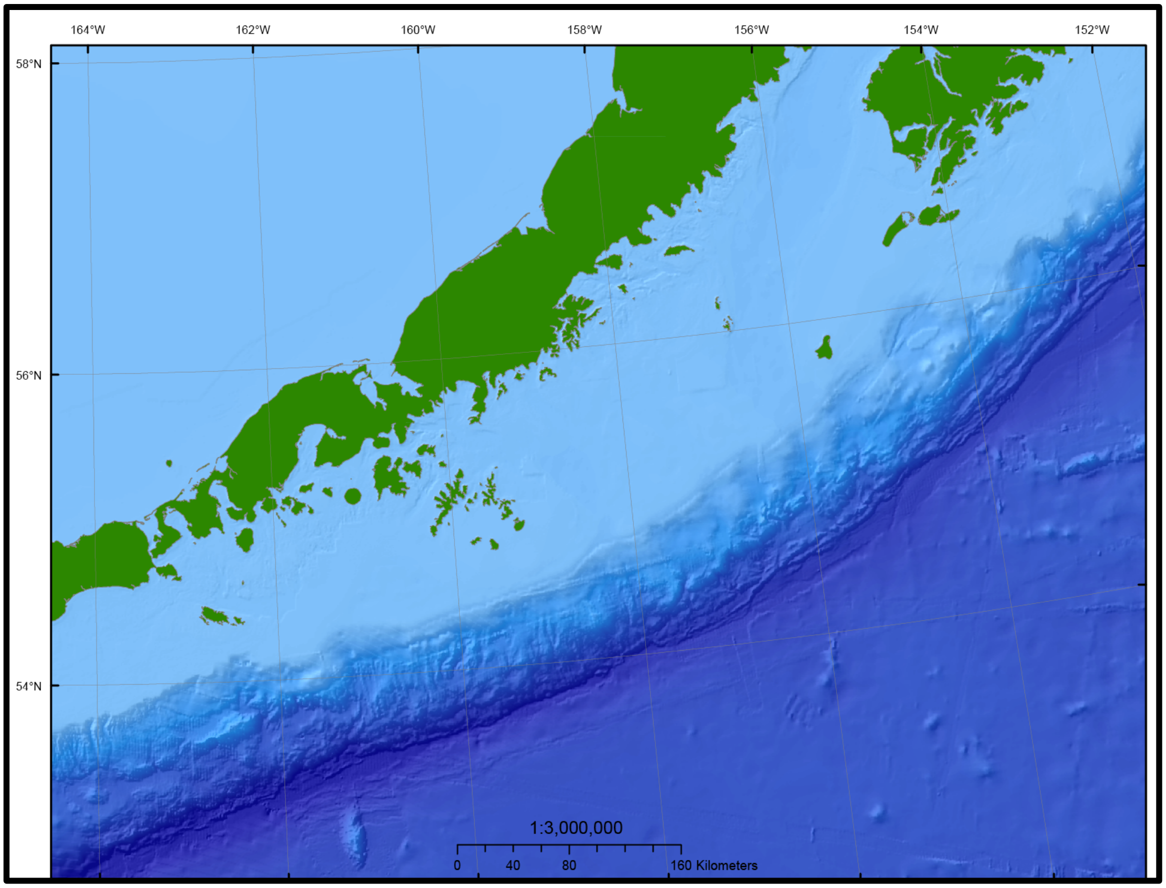
164°W
162°W
160°W
158°W
156°W
154°W
152°W
58°N
56°N
54°N
1:3,000,000
0
40
80
160 Kilometers

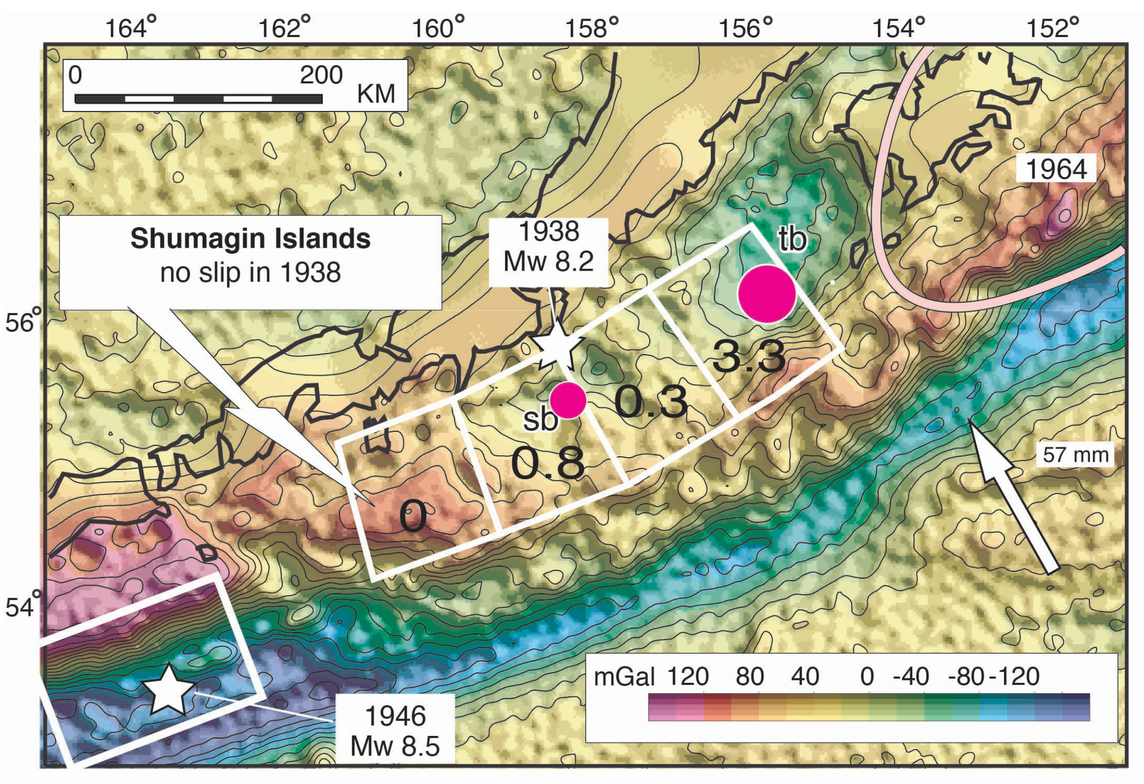
164°
162°
160°
158°
156°
154°
152°
56°
54°
0
200
KM
Shumagin Islands
no slip in 1938
1938
Mw 8.2
tb
sb
0
0.8
0.3
3.3
1964
57 mm
1946
Mw 8.5
mGal 120 80 40 0 -40 -80 -120

Figure 3. Maps showing bathymetry and free-air gravity of a part of the Alaska Peninsula subduction margin. *A*, Color shaded relief map of the bathymetry of the southwest half of the Alaska Peninsula (data source, National Geophysical Data Center; map construction by Holly Ryan). Parallel ridges northwest of the otherwise flat-bottomed trench are largely a consequence of active thrust faulting, folding, and slumps in the outer prism. *B*, Free-air gravity reveals structural highs and lows (basins) along Semidi Islands segment and likely show the extent of framework basement rock southeastward to the strong gradient along the trench (Wells and others, 2003). The locations where significant slip occurred in 1938 (white rectangles), average 1938 slip in meters (black labels), and high moment release in 1938 (red circles) are from Johnson and Satake (1994) and Estabrook and others (1994). These features suggest that not only was the slip release small in the 1938 event (~2 m, see text), but also the updip sector of the subduction boundary may not have ruptured significantly in 1938.

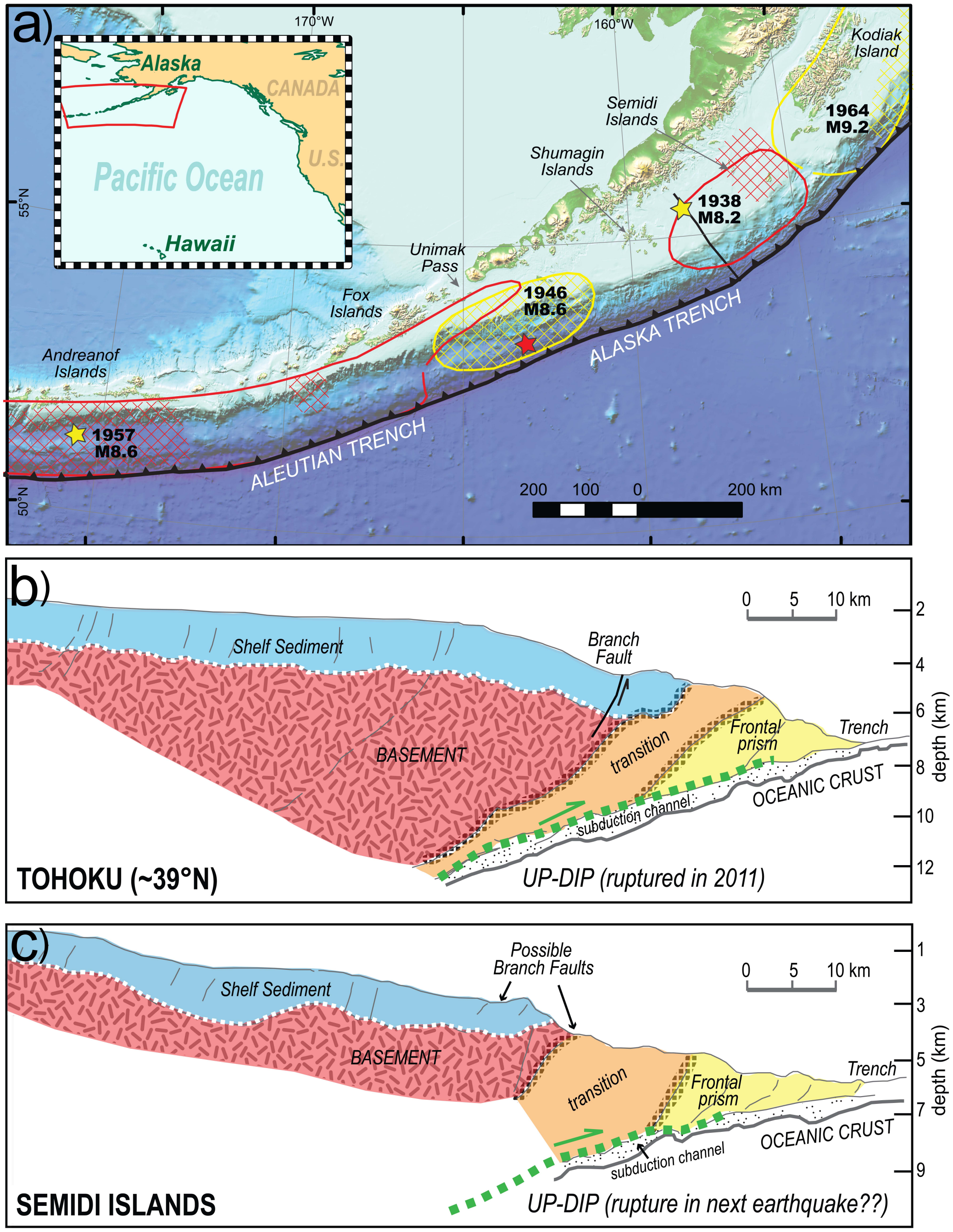

Figure 4. Map of the Alaska margin and cross sections of both the Alaska and Tohoku, Japan, subduction margins. (Figure and caption modified from Ryan and others, 2012a.) a, The Alaskan margin showing epicenters (stars), rupture zones (red and yellow outlines), and areas of largest slip (greater than 3 m, red and yellow cross-hatching) of instrumentally recorded large earthquakes. Black line with barbs shows the location of the Alaskan- Aleutian subduction zone's main trench on the sea floor. b, Structure section across the similar Tohoku margin crossing the north end of the Tohoku earthquake rupture (after von Huene and others, 1994). c, Structure section across the 1938 epicenter near Semidi Islands, located in figure 4a

(from von Huene and others, 2012). In both profiles framework crust extends nearly to the trench. A transition zone between basement and frontal prism material is poorly imaged—better characterization of these zones will help assess hazards. The dashed green lines show the border between the downward dipping subducting slab and the continental crust thrusting over it

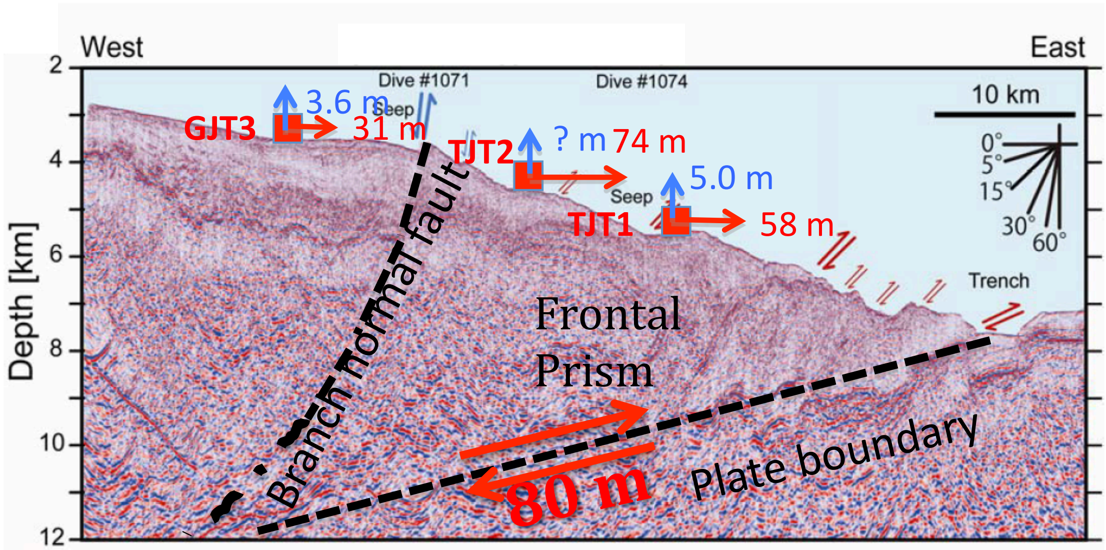

Figure 5. Seismic-reflection survey cross-section image perpendicular to the Japan Trench near 38°N acquired before the 11 March 2011 Tohoku-oki earthquake, with arrows showing the horizontal (red arrows) and vertical (blue arrows) motions of sea-floor instruments during the earthquake. Modified from Ito and others (2011). The motions of the sea-floor instruments are consistent with an average of 80 m of coseismic slip under the frontal prism. Note the normal fault branching off the plate-boundary fault that is thought to represent the kinematic accommodation of such a steep downdip gradient in slip on the subduction boundary. Angular scale in upper right shows the true dip angles.

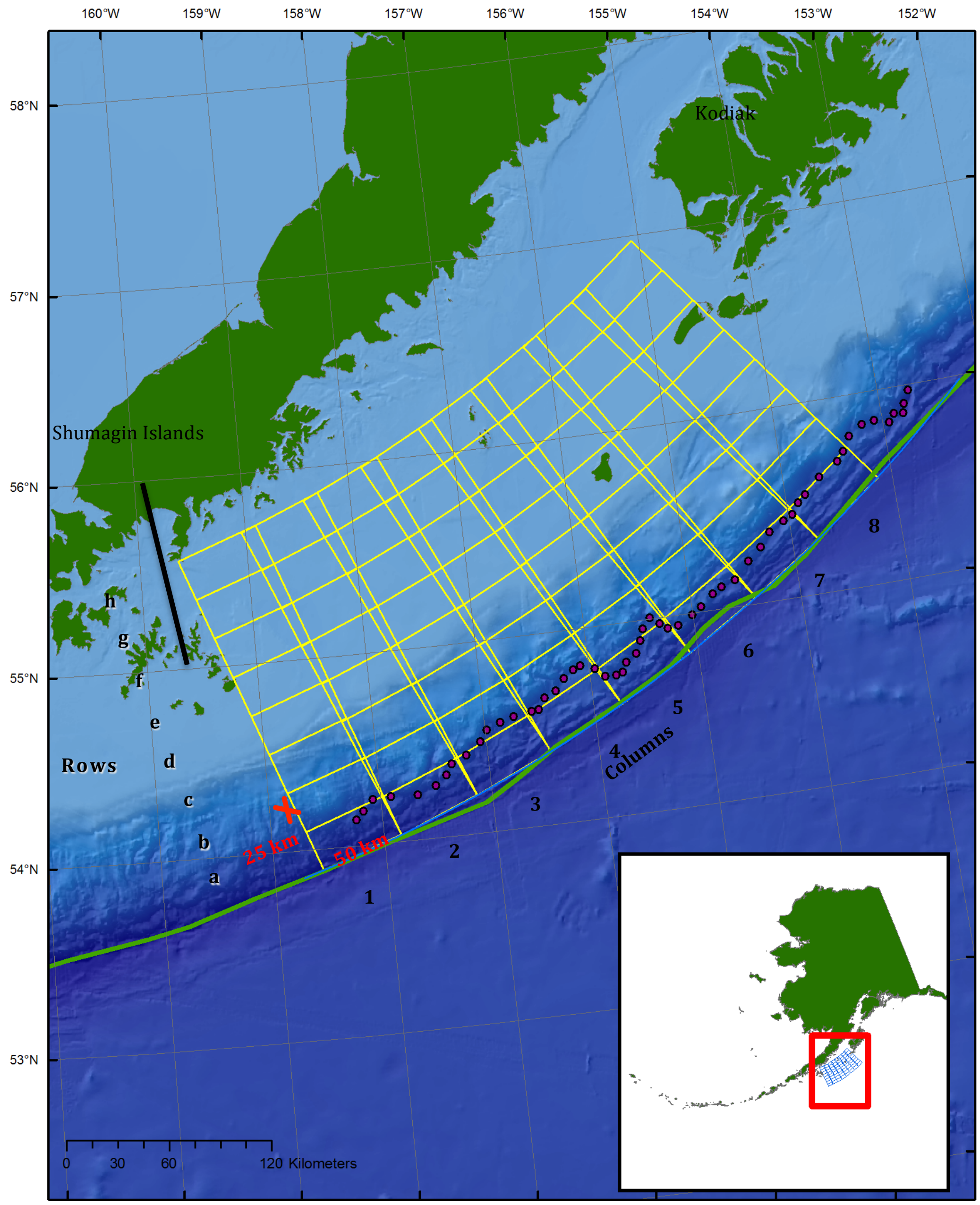

Figure 6. Map of the initial surface subfault grid of 25×50 km cells adapted to the Semidi subduction sector bathymetry off the Alaska Peninsula. Each subfault area is identified and labeled by the row and column in the subfault grid where it is located. Unwanted overlaps between adjacent subfaults are eliminated graphically in figure 7. Red dots indicate the boundary of the frontal prism as picked by Roland von Huene. Color shaded relief from National Geophysical Data Center.

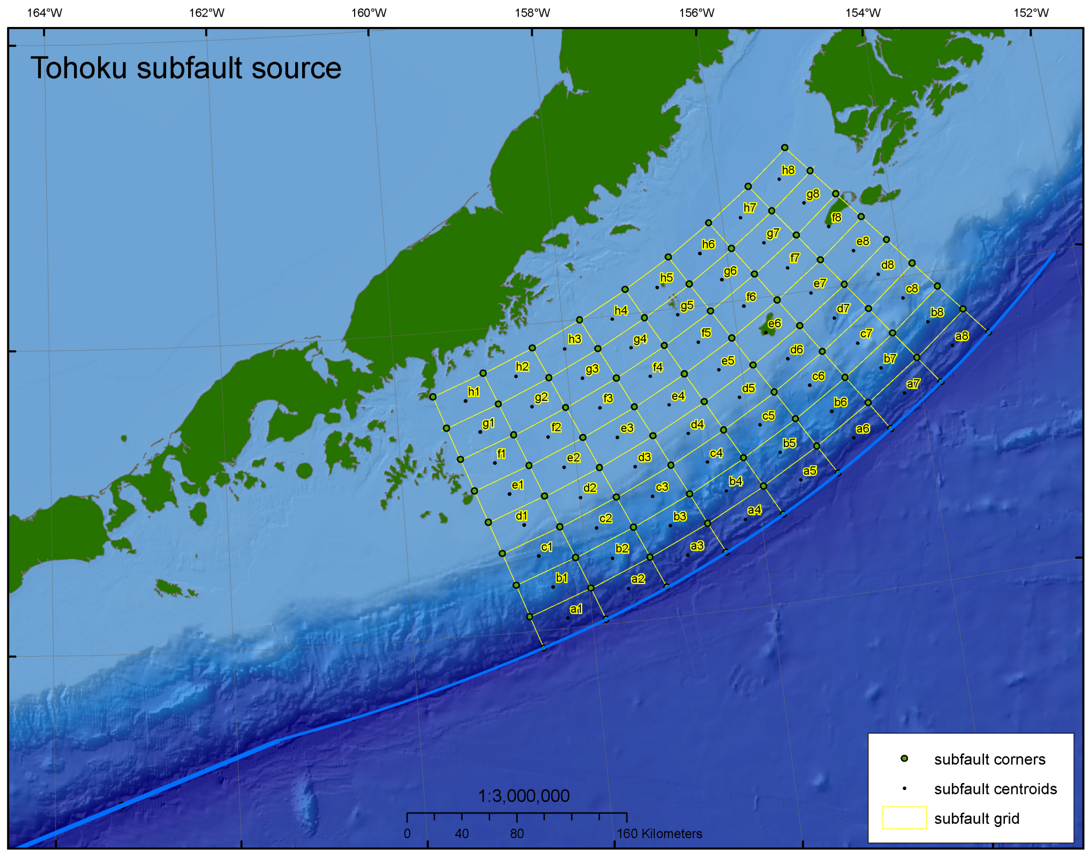

Figure 7. Map showing final surface projection of subfault grid in the Semidi sector, with subfault boundary overlaps removed and matrix subfaults labeled.

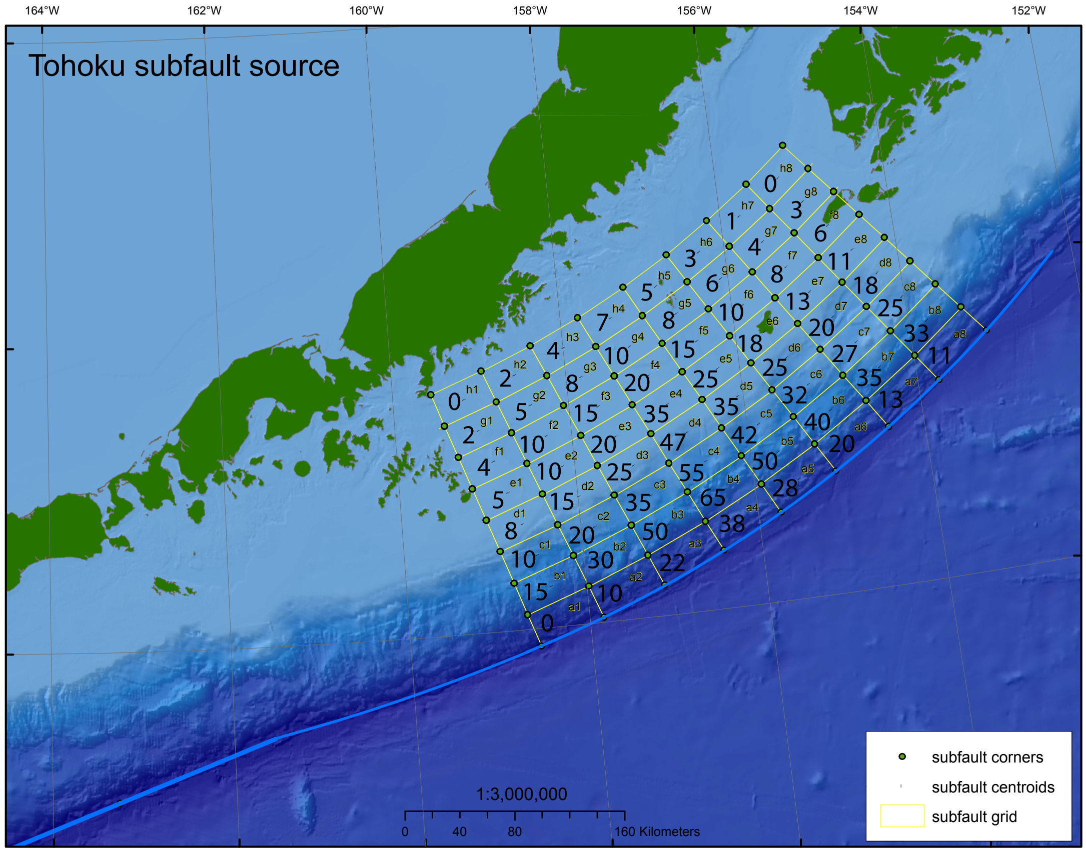

Figure 8. Map of the final 3-D subfault grid of the Semidi sector, with posited seismic-slip distribution in meters (red labels) based on a synoptic summary of the Mw 9.1 Tohoku earthquake slip models. Depth contours on subduction boundary (based on Slab 1.0) are shown in yellow.

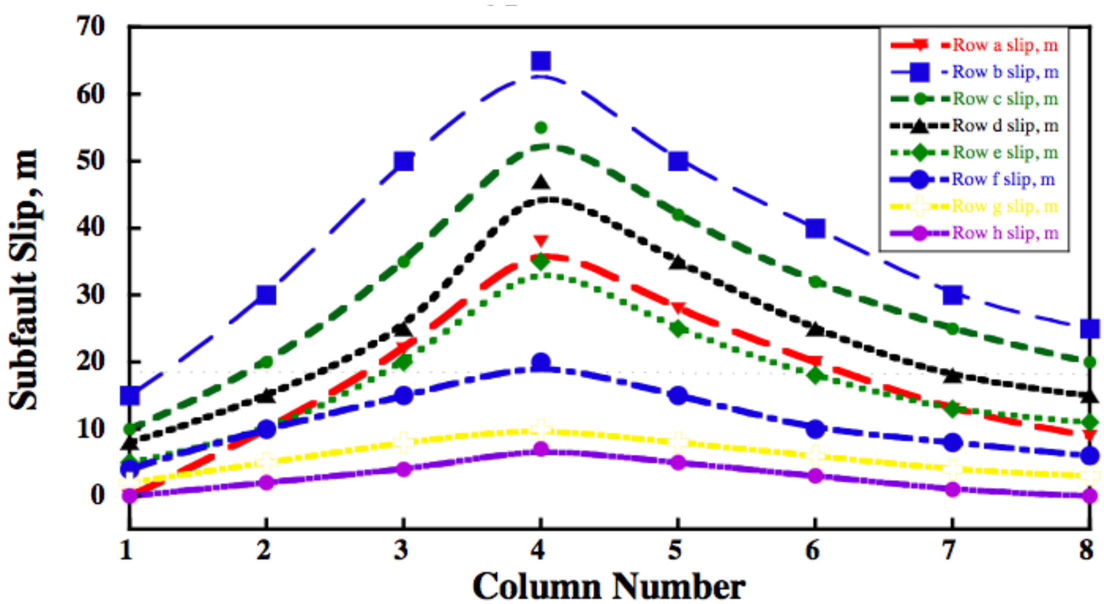

Figure 9. Plotted trench-parallel profiles of seismic slip in subfault rows of the Semidi sector grid at increasing distances from the Alaska Trench (row "a" is closest to the trench).

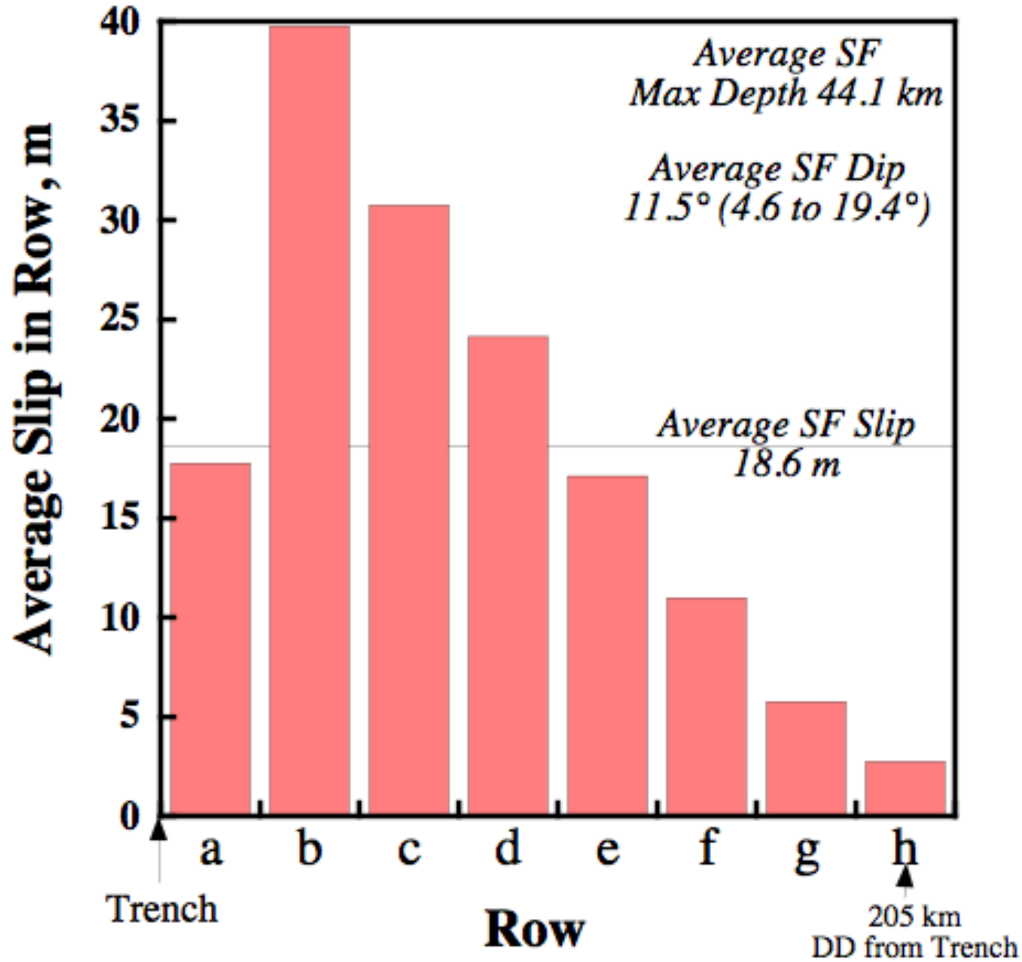

Figure 10. Histogram showing average slip in subfault rows of the Semidi sector grid parallel to the Alaska Trench. SF is subfault. DD is downdip.

Appendix. Supplementary Information

Table A. Spreadsheet summarizing the subfault geometry and slip distribution for the SAFRR Southern California Tsunami Scenario [See the accompanying file].